Swiss Journal of Geosciences (2018) 111:475–500
https://doi.org/10.1007/s00015-018-0311-x

Dolomitization of the Upper Jurassic carbonate rocks in the Geneva Basin, Switzerland and France

Yasin Makhloufi[1] · Elme Rusillon[1] · Maud Brentini[1] · Andrea Moscariello[1] · Michel Meyer[2] · Elias Samankassou[1]

Received: 1 September 2017 / Accepted: 1 May 2018 / Published online: 30 May 2018
© Swiss Geological Society 2018

Abstract
The Upper Jurassic carbonates represent important potential targeted reservoirs for geothermal energy in the Geneva Basin (Switzerland and France). Horizons affected by dolomitization, the focus of the present study, are of particular interest because they proved to be productive in time-equivalent deposits currently exploited in Southern Germany. The study is based on sub-surface samples and outcrops in the Geneva Basin. Petrographic analyses allowed to constrain the paragenesis of the Upper Jurassic units prior to discussing the cause(s) and effect(s) of dolomitization. Data reveal that the facies are affected by early and late diagenesis. All samples show at least two stages of burial blocky calcite cementation with the exception of those from the sub-surface, which display an incomplete burial blocky cementation preserving primary intercrystalline porosity. Dolomitization affected all units. The results point to an early dolomitization event, under the form of replacement dolomite. Dedolomitization, through calcitization and/or dissolution, is an important process, creating secondary pore space. Results of the present study favor a reflux model for dolomitization rather than the mixing-zone model suggested in earlier work. However, considering the geodynamic context, other dolomitization models cannot be excluded for the subsurface. The presence of secondary pore space might contribute to the connectivity of the porous network providing enhanced reservoir properties. These results are a first step towards a better understanding of the diagenetic history of the Upper Jurassic in the Geneva Basin. Moreover, it provides a reasonable framework for further geochemical analyses to constrain the nature and timing of fluid migration. The paragenesis and the dolomitization model hold the potential to help in ongoing exploration for geothermal energy beyond the Geneva Basin.

Keywords Geneva BasinKimmeridgianDiagenesisDolomitizationDedolomitization

1 Introduction

In a world where the demand for fossil and renewable energy continues to rise, reservoir characterization and modeling is an essential step for the better management of resources. The reservoir properties of carbonates have been well studied in the past but still represent a challenge as limestones are strongly affected by diagenetic alteration. The heterogeneity of reservoir properties in carbonate rocks (e.g., Westphal et al. 2004; Davis et al. 2006; Dou et al. 2011) can be explained by (1) the fracturation leading to non-matrix flow network and (2) the complex diagenetic path of the reservoir (Walls and Burrowes 1985; Machel 1987; Mountjoy and Marquez 1997; Wilson and Evans 2002; Ehrenberg and Nadeau 2005; Rong et al. 2012). It is therefore difficult to understand and to predict the distribution of petrophysical properties in carbonate reservoirs. The GEothermy 2020 (GEo2020) program aims at exploring and eventually exploiting the deep geothermal resources of the Geneva Basin (GB). Based on a 3-D geological model of the Greater Geneva Basin combined with petrophysical data (Clerc et al. 2015), five units were targeted as potential reservoirs in the Lower Triassic (Bundsandstein and Muschelkalk), the Middle Jurassic (Bajocian), the Upper Jurassic (Kimmeridgian), and the Early Cretaceous (Barremian). This study focuses on the

Editorial handling: S. Spezzaferri.

✉ Yasin Makhloufi
yasin.makhloufi@unige.ch

[1] Department of Earth Sciences, University of Geneva, Rue des Maraîchers 13, 1205 Geneva, Switzerland

[2] Service Industriels de Genève (SIG), CP 2777, 1211 Geneva, Switzerland

Upper Jurassic deposits well characterized in the past by numerous sedimentological and stratigraphic studies (e.g. Deville 1988, 1990; Fookes 1995; Charollais et al. 1996, 2013; Mouchet 1998; Gygi 2013; Rameil 2008; Strasser et al. 2015). The Upper Jurassic and, specifically, the Kimmeridgian limestones are known to be affected by dolomitization (Fondeur et al. 1954). Dolomitization is commonly associated with important modifications of the reservoir properties by poro-genesis or poro-necrosis mechanisms (Schmoker et al. 1985; Braithwaite 1991; Giorgioni et al. 2016). However, the paragenesis of the Kimmeridgian is poorly constrained in the GB, and dolomitization processes remain not well understood. The dolomitization model currently available is the one by Fookes (1995), following the interpretation made in Bernier (1984), and which proposed a mixing-zone (i.e., the mixing of phreatic seawater with meteoric waters) model to explain the dolomitization in this area. The mixing-zone dolomitization scenario has been the subject of many discussions among the scientific community in the last decades, mainly due to the fact that dolomitization depends on the stoichiometry of the reaction, the temperature, and the fluid composition. It is now accepted that the requirement in terms of volume and Mg concentration of fluid necessary for a mixing-zone dolomitization of large sedimentary bodies cannot be met (Warren 2000; Machel 2004).

Based on field analogs and subsurface data, the present study aims to provide a paragenetic framework for the Kimmeridgian in the GB and to discuss the potential dolomitization scenarios. Dolomitic fabrics and dolomitization processes from time-equivalent deposits reported in the literature are reviewed and compared with results from the present study. Furthermore, the impact of dolomitization on reservoir quality in the Upper Jurassic of the GB is evaluated with respect to possible future geothermal exploration of the GB.

2 Geological context and study sites

2.1 Geological setting

The Greater Geneva Basin is located at the Swiss-French transnational zone in the south-west of Lake Geneva. The basin is limited to the north-east by the internal chain of the Jura Mountain and to the south-east by the front of the Alpine units (Fig. 1). The basin has a Variscan crystalline basement covered by 3000–5000 m thick Mesozoic to Cenozoic successions. The Mesozoic series are mainly composed of carbonates and marls, along with evaporites. The Triassic is marked by a marine transgression during which the basin was connected to the Tethys Ocean, leading to the deposition of thick evaporitic series (Disler 1914). While the Lower Jurassic sediments are still influenced by the marine transgression, two successive regressive trends affect the Middle and Upper Jurassic series. Open-marine conditions prevailed from the Hettangian until the Toarcian, shifting to shallower conditions during the Bajocian and Bathonian. A shallow carbonate platform developed during the Upper Jurassic, extending towards the north-west until the early Cretaceous. During the Kimmeridgian patch reefs developed on top of pre-existing structural highs (Meyer 2000). The sealing of inter-reef depressions by prograding tidal deposits followed during the Tithonian, with the local occurrence of immersive facies (Strasser 1994).

The Kimmeridgian and Tithonian sequences of the GB can be subdivided into four major units: the *Couches à Céphalopodes*, the *Calcaires de Tabalcon*, the *Complexe Récifal*, and the *Tidalites de Vouglans* (Fig. 1). The *Complexe Récifal* is subdivided in three subunits: the *Calcaires Récifaux*, *Calcaires Plaquetés*, and *Calcaires de Landaize* subunits. The *Couche à Céphalopodes* unit was deposited in a deep open marine environment and is mainly represented by marly limestones with a thickness of 100 m. The unit consists of meter-thick interbeds of fine grey to beige limestones and marly beige limestones. The fauna consists of ammonites, belemnites, and thin bivalves. This unit is dated as early to late Kimmeridgian (Enay 1969; Bernier and Enay 1972; Bernier 1984). The thin-bedded limestones consist of mudstone rich in organic matter and pyrite, along with rare oncoids and glauconite. Bioclasts are composed of echinoderms (echinoids, ophiuroids, holothurians), sponge spicules, bivalves, and serpulids. The *Calcaires de Tabalcon* unit is characterized by several decimeter-thick beds, about 20-m thickness, exhibiting discrete bedding. The facies is coarsening up with fine micritic limestones including sparse bioclasts at the base to a tight bioclastic limestone with debris originating from the dismantlement of a carbonate platform with corals, diceratids, pectinids, rare bivalves, gastropods, and crinoid ossicles. Locally, silica can be observed, likely remains of sponges. The upper part of the *Calcaires de Tabalcon* is affected by dolomitization. The *Complexe Récifal* forms a discontinuous white unit of variable thickness (Deville 1988). In the Vuache Mountains, Charollais et al. (2013) estimate a maximum thickness of about 200 m. The *Calcaire Récifaux* unit consists of a compact white limestone with facies associations typical for coral dominated reef environment: bindstones (including intervals rich in microbialites), mudstones, and rudstones. The *Calcaire Plaquetés* unit consists of thin-laminated beds rich in bitumen, gypsum, halite, and dolomite. Laterally, this unit varies significantly in thickness reaching up to 200 m to compensate depressions between reef bodies of the *Calcaire Récifaux* unit.

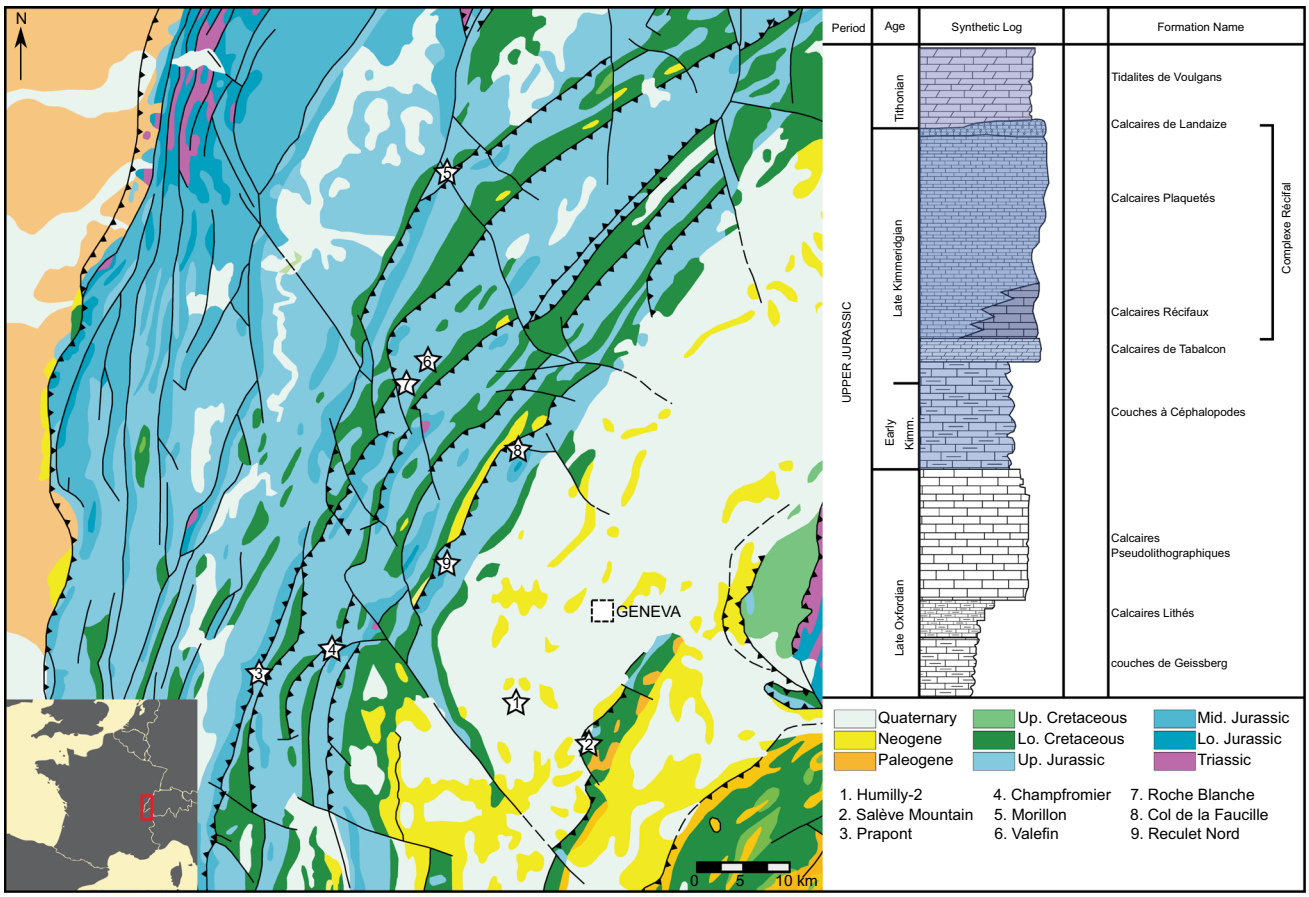

Fig. 1 Simplified geological map of the study area, with the location of the study sites, and a synthetic log of the Upper Jurassic units as exposed in Mount Vuache Modified from Charollais et al. (2013)

The *Calcaire Plaquetés* unit was deposited in inter-reefal settings and could fill up all available space between the *Calcaire de Tabalcon* and the *Tidalites de Vouglans* formations. The *Calcaire de Landaize* unit is composed of bioclastic grainstone including coral fragments, stromatopores, echinoderms, and gastropods corresponding to a shallow lagoon with high-energy conditions. This unit consists of 0.2–2.5 m-thick beds with a maximum thickness up to 15 m. The *Tidalites de Vouglans* unit is composed of less than a meter thick limestone beds and marly to dolomitic interbeds. The dominant facies is a white to grey mudstone rich in pyrite, locally including microbial mats and mud cracks indicative of a foreshore tidal environment (Strasser 1994).

During the Early Cretaceous, overall shallow and warm-water conditions prevailed (Debelmas and Michel 1961; Sommaruga 1997; Charollais et al. 2013) leading to the deposition of bioclastic limestones, bioturbated limestones, and organic-rich marls. Upper Cretaceous deposits are not recorded in the GB, probably due to the late Cretaceous emersion and later erosion during the Early Cenozoic. This erosion led to the development of an important karstic system that was filled during the Eocene by the so-called "sidérolithique", a red sandstone formation (Debelmas and Michel 1961). The Alpine orogeny and the associated development of the foreland basin induced the deposition of a thick Oligocene–Miocene detritic Molasse unit (Favre et al. 1880; Heim 1922; Charollais et al. 2007).

2.2 Study sites

The Kimmeridgian units in the GB were studied in one borehole and several outcrops across the basin (Fig. 1). Sedimentologic logs of the Saleve, Reculet, and Prapont sections as well as the Humilly-2 well are summarized in Fig. 2. In the south-eastern part of the basin, the *Calcaire de Tabalcon* unit was studied along the Etiollets section at the Salève Mountain (Fig. 2a). This outcrop was described by Deville (1988, 1990). Field data and sedimentologic interpretations were published in previous works (Joukowsky and Favre 1913; Carozzi 1950, 1954, 1955). Deville (1988) described four different facies: one micritic, two bioclastic and one dolomitized facies. The northern part of the basin is studied in several outcrops of the Folded Jura: Le Reculet Nord, Morillon, Valefin, Roche Blanche, and Le Col de la Faucille. The Reculet Nord section starts

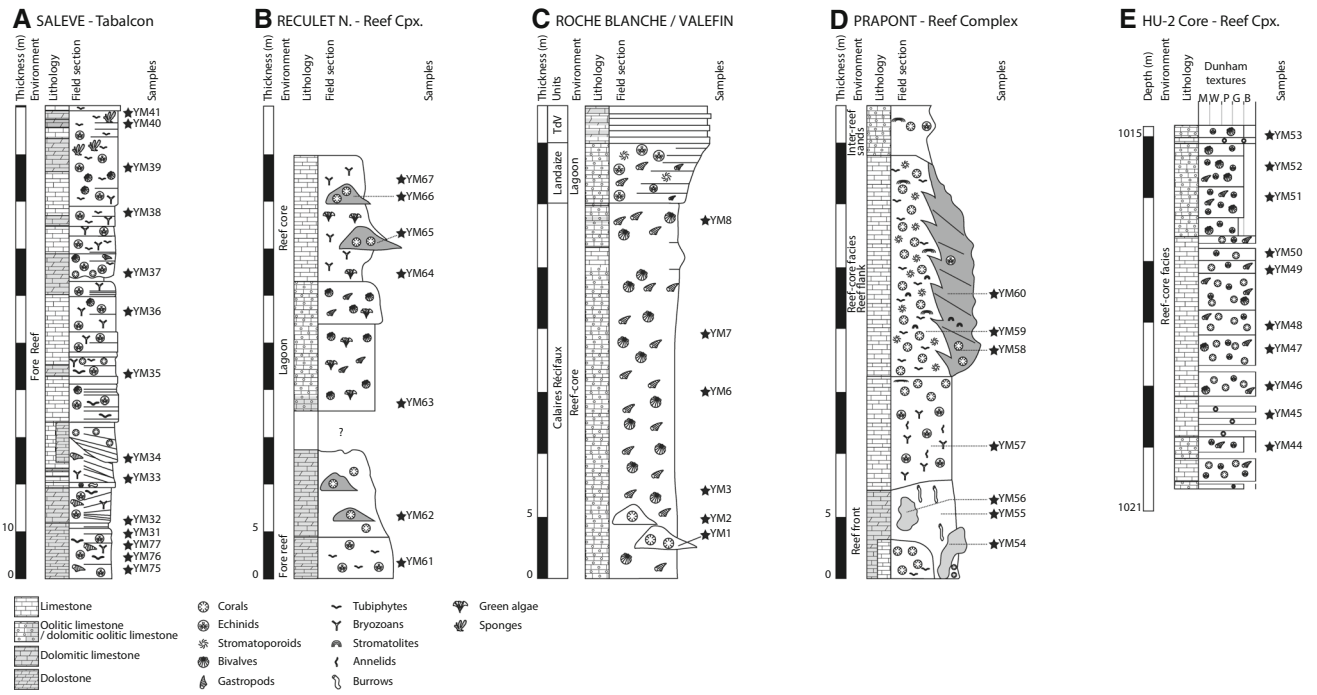

Fig. 2 Sedimentologic logs for: **a** the *Calcaires de Tabalcon* unit the Salève Mountains, modified from Deville (1990). **b** The top of the *Calcaires de Tabalcon* and the *Calcaires Récifaux* in the Reculet Nord section, modified after Meyer (2000). **c** the *Calcaires Récifaux, Calcaires de Landaize* and *Tidalites de Vouglans* (TdV) unit in the Roche Blanche and Valefin sections. **d** The reef-front and reef-core sections of the *Calcaires Récifaux* in the Prapont section, modified from Fookes (1995). **e** Description of the 5 meters core available in the Humilly-2 well, representing the top of the *Calcaires Récifaux* unit. Stars indicate collected samples with sample labels

with the top of the *Calcaires de Tabalcon* unit (Fig. 2b) overlain by the *Calcaires Récifaux* unit (Fig. 2b). This section was previously described by Meyer (2000). The Rocher du Morillon is a succession of about 70 m of tectonically verticalized to sub-verticalized limestone beds, marly limestones, and marl beds in an anticlinal structure called *Les Planches*. Approximately 20 km south of Morillon, along the road D437, following the Foulasse and Bienne rivers, the *Calcaires Récifaux*, *Calcaires de Landaize*, and *Tidalites de Vouglans* units outcrop in Valefin Lès Saint-Claude and Roche Blanche (Fig. 2c). The *Calcaires de Landaize* outcrop in the Col de la Faucille section, a mountain pass above the city of Gex accessible by the N5 road in the direction of Les Rousses.

The *Calcaires Récifaux* unit outcrops in the western part of the basin in Prapont and Champfromier. The Prapont section was well described by several authors (Pelletier 1953; Enay 1965; André 1962) and more recently in Fookes (1995). The outcrops are characterized from its base to the top by subtidal deposits followed by reef front deposits, a first reef sequence, inter-reef sands making the transition towards a second reef sequence on which lagoonal and subtidal storm deposits are found (Fookes 1995). Sampling focused on the reef front and first reef sequence, which is affected by dolomitization, and include numerous vuggy pores (Fig. 2d). Ten kilometers east from the Prapont section, the Champfromier section can be studied along the road D14 towards the village of Forens. The outcrop, described by Bernier (1984), consists of thick limestone beds with a regular dip of about 20° towards the east.

Subsurface data originates from the Humilly-2 well (Fig. 1) located in the center of the GB in the French department of Haute-Savoie. This well currently serves as a reference for the subsurface characterization of the GB (Clerc et al. 2015; Moscariello 2016; Rusillon et al. 2016). Stratigraphical and lithological control on the sedimentary units of HU-2 is provided by the outcrops in the Jura Mountains, Mount Vuache, and Mount Salève (from the Upper Triassic to the Quaternary). Only one core section including the Kimmeridgian was retrieved from 1021 to 1015 m, and is described in Fig. 2e. No sedimentological logs are drawn for the Morillon, Col de la Faucille, and Champfromier sections as they display virtually no variations in terms of facies.

3 Sampling strategy and analytical methods

At Mount Salève, 14 samples were taken along the path exposing the *Calcaires de Tabalcon* unit. Sample selection was tied to data from the stratigraphic section measured by

Deville (1988) (Fig. 2a). In Champfromier, seven samples were taken along the outcrop. In the Folded Jura, 16 samples were studied: two in Morillon, three in Valefin, three in Roche Blanche, two in the Col-de-la-Faucille area, and seven in the Reculet Nord (Fig. 2b, c). In the Prapont section, seven samples were taken: three in the dolomitized reef front deposits and four in the first reef sequence following the scheme of Fookes (1995; Fig. 2d). Ten samples were taken from the HU-2 well, every 50 cm (Fig. 2e), in addition to those originating from the study by Rusillon et al. (2016). Core samples were taken directly from the core as plugs with a diameter of 25 mm. Samples from outcrops and cores were prepared for thin section analysis. Thin sections, impregnated with epoxy resin stained by Methylene blue, were used to define the texture, grain type, bioclast content, grain size, mineralogy, cement type, and pore-type distribution. Cathodoluminescence analysis was completed using an ERI-MRTech-optical cathodoluminescence microscope with a cold cathode mounted on an Olympus BX41 petrological microscope (Department of Earth Sciences, University of Geneva, Switzerland). The beam conditions were 15–18 kV at 120–200 mA with an unfocused beam of approximately 1 cm. Carbon coating (ca. 15 nm) by carbon thread evaporation was used prior to imaging with the Jeol JSM 7001F Scanning Electron Microscope (SEM, Department of Earth Sciences, University of Geneva, Switzerland). Semi-quantitative analyses and mapping were obtained with an EDS detector coupled with the JED 2300 software. Calcite staining (Dickson 1966) was performed to constrain the cement mineralogy and the paragenesis.

4 Petrography

4.1 *Calcaires de Tabalcon* unit

The *Calcaires de Tabalcon* displays four distinct sedimentological facies in the Etiollets section. The first facies is micritic with the accumulation of micropeloids and a faunal association typical for open-marine, low-energy, outer shelf environments. This facies is intensively dolomitized. Blocky calcite displays a dull luminescence with zonations (Fig. 3a, b). Dolomite is composed of fine to medium, euhedral planar-porphyrotopic, replacive rhombs. Crystals are generally displaying a cloudy core and a clear rim. The dolomite has a non-luminescent dark center surrounded by dull luminescent red zones toward the borders (Fig. 3a, b). The dolomite rhombs exhibit selective dissolution and calcitization along their core/rim interface (Fig. 3d), associated with intracrystalline microvugs. Dolomite rhombs are partly dissolved along younger stylolites (Fig. 3b). The second facies is bioclastic with wackestone and packstone to grainstone textures. The third one is lithoclastic. In both facies, two phases of calcite cements are observed: (1) syntaxial overgrowth around echinoderm fragments and (2) blocky calcite cementation filling the available inter-particular pore space. Under CL, the blocky calcite shows a dull luminescence with orange to brown zonations. Both facies are often affected by fractures sealed by sparitic calcite exhibiting a bright yellow to brown luminescence. Dolomite rarely occurs in these facies. The bindstone facies is composed of siliceous sponges including pyrite-limonite and is characterized by two stages of blocky calcite cementation (Fig. 3e–f): the first displaying a non-luminescent core with yellow bright luminescent zonations and the second marked by a bright yellow luminescence with zonations under CL. Two stages of dolomitization can be distinguished (Fig. 3e–f): (1) fine idiotopic, euhedral clear rhombs displaying a red bright luminescence and intersecting the blocky calcite cementations (dolomite 1) and (2) fine to medium euhedral to subhedral rhombs with cloudy cores and displaying a mauve bright luminescence, intersecting the first stage (dolomite 2). Both exhibit thin zonations under CL. Both stages of dolomites exhibit dedolomitization by calcitization. The dolomite is intersected by micro-fractures filled by calcite that is yellow bright luminescent under CL.

In the Reculet Nord section, the *Calcaires de Tabalcon* is characterized by a dolomitized micritic limestone consisting of medium to coarse, euhedral, highly coalescent replacive rhombs that obliterated the initial fabric. Most of the rhombs display a dark cloudy core and clear outer rim (Fig. 3g). Under CL, the rhombs display a thick dull luminescent orange to brown-zoned core evidencing dissolution and mauve to pink dull luminescent zoned rims (Fig. 3h). The zoned rims form syntaxial overgrowth on crystal facing pores.

4.2 The Reef Complex unit—*Calcaires Récifaux*

The Upper Jurassic is about 800 m thick (non-published final drilling report of the HU-2 well) and can be subdivided in two units: a lower marly limestone unit (from 1855.6 to 1644 m) and an upper limestone unit (from 1644 to 812 m). The upper limestone unit includes the interval dated as Kimmeridgian (from 1271 to 846 m) with an unidentified lower limit. Several lithologies were observed from the base to the top: 153 m of beige limestone with evidences of sucrosic dolomite; 73 m of crystalline to micro-crystalline white limestone; 36 m of white chalky limestone; 60 m of beige oolitic grainstone and dolomitic limestone and 103 m of white limestone, often chalky, coarse, and oolitic. The *Calcaires Récifaux* unit in HU-2 consists of a white bioclastic limestone composed of gastropods, brachiopods, corals, echinoderms, and

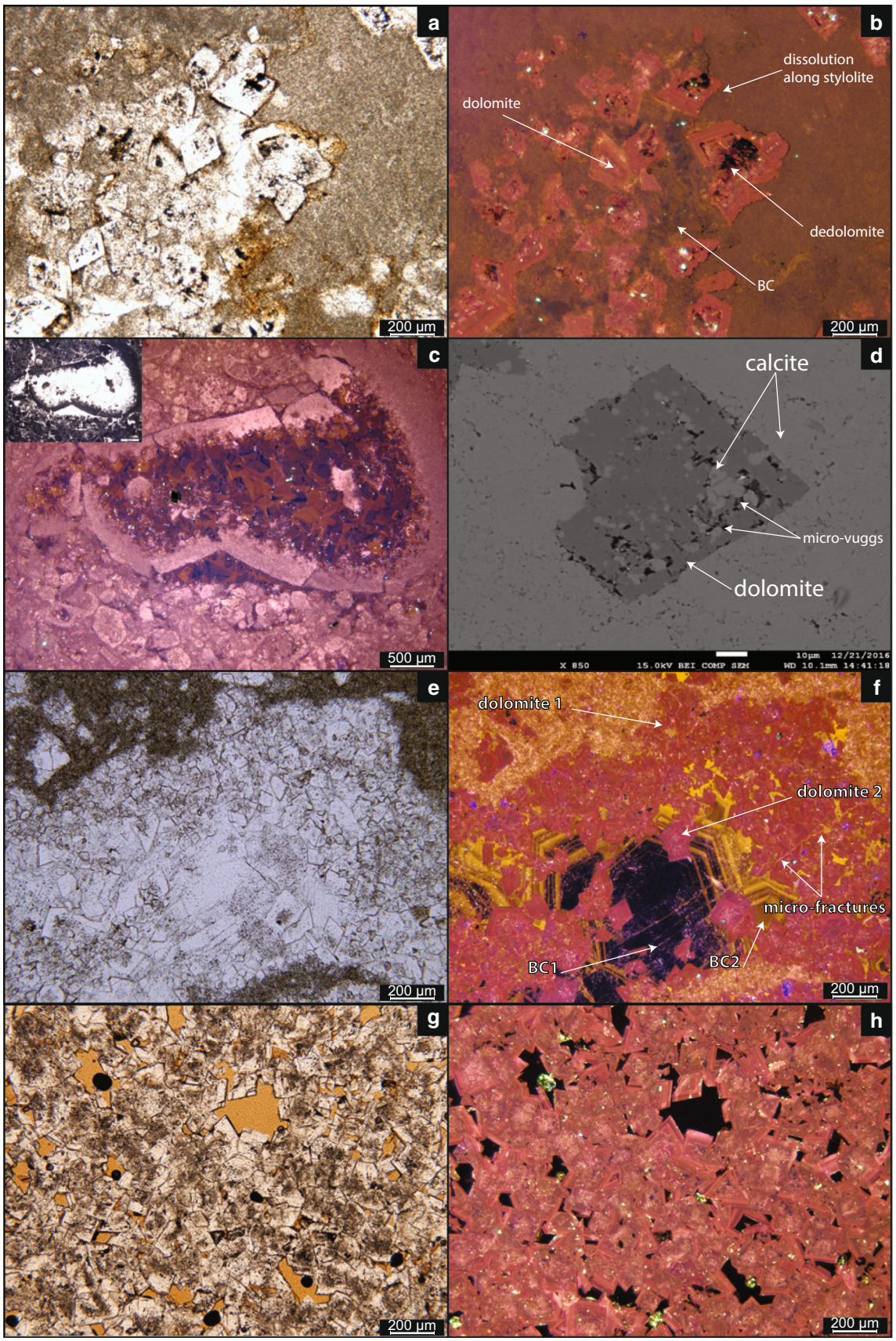
a
200 µm
b
dissolution
along stylolite
dolomite
dedolomite
BC
200 µm
c
500 µm
d
calcite
micro-vuggs
dolomite
X 850 15.0kV BEI COMP SEM 10µm 12/21/2016 WD 10.1mm 14:41:18
e
200 µm
f
dolomite 1
dolomite 2
micro-fractures
BC1
BC2
200 µm
g
200 µm
h
200 µm

◀**Fig. 3** Photomicrographs (optical microscope and cathodoluminescence) of the *Calcaires de Tabalcon* unit. **a**, **b** Dolomitized and dedolomitized mudstone and late stylolithization in natural light and cathodoluminescence. Blocky calcite (BC) exhibits dull luminescence under CL (sample YM32). **c** Bioclast affected by compaction exhibiting two stages of blocky calcite cementation (BC1 and BC2, sample YM34). **d** SEM photograph of dedolomite composed of remaining dolomite and microvugs filling calcite (sample YM77). **e**, **f** Planar euhedral dolomite overprinting blocky calcite cementation (BC), in natural light and cathodoluminescence (sample YM40). **g**, **f** Sucrosic dolomite with cloudy cores and limpid rims, natural light and cathodoluminescence (sample YM61)

foraminifers. The majority of the core is composed of bindstones, rudstone, and grainstone in the first meter at the top of the core. Centimetric vugs are mostly associated with the presence of corals. Using CL, several stages of calcite cementation were identified in thin sections: (1) an isopachous cement rim around allochems, (2) syntaxial overgrowth around echinoderms, (2) three different stages of blocky calcite cementation filling the available interparticular pore space (Fig. 4a, b). The first stage of blocky calcite cementation exhibits a dull brown luminescence under CL followed by a second mainly non-luminescent stage with bright yellow zonations. The third stage of blocky calcite cementation shows a dull to bright luminescence with orange to brown colors. Locally, this late stage of cementation is incomplete with intra-crystalline pores preserved (Fig. 4b). Only one sample (1020.5 m) displays dolomite after calcite staining.

In the Prapont section, the reef front deposits exhibit beige wackestone with microsolenoid corals, stromatoporoids, bryozoans, and rare foraminifers, along with oncoids and micropeloids associated with microbial crusts. Lateral variations at small scale are important in these deposits with locally dolomitized patches. Some of these patches are intensively bioturbated. Moldic and intergranular porosity as well as cm- to dm-size vuggy pores are common. Samples from the reef front consist of micritic limestone with large sparitic cements and rhombohedral pores (Fig. 4c, d). Under CL, the sparitic calcite displays a dull orange to brown luminescence with zonations. The rhombohedral pores are partially filled by de-dolomite with a dull to bright red luminescence (Fig. 4c, d). The Valefin and Roche Blanche outcrops consist of a set of bioherms at the base that are more resistant to erosion. These bioherms are composed of white limestone units rich in rudists and corals, separated by an oolitic grainstone with occurrences of nerinids and rudists. This grainstone is cemented at various degree and can exhibit partial interparticular moldic porosity. Samples exhibit rare vugs filled by blocky calcite cements (Fig. 4e) displaying a dull luminescent core followed by bright luminescent orange zones. Two stages of dolomitization can be distinguished (Fig. 4e, f): (1) very fine euhedral, pervasive replacive clear rhombs and (2) medium euhedral, pore ceiling, clear rhombs with cloudy cores and displaying a mauve bright luminescence, intersecting and surrounding vug-filling blocky calcite cements. Both exhibit a bright to dull luminescent yellow to orange-zoned core transitioning to thin red luminescent-zoned rimes (Fig. 4f).

The *Calcaires Récifaux* unit in the Champfromier section is characterized by micritic limestone including rare fragments of brachiopods, echinoderms, bivalves, and green algae. The limestone is intensively affected by fractures and micro-fractures filled by sparitic calcite displaying twining. Under CL, the calcite infilling of fractures is characterized by an orange to brown dull luminescence with zonations. This stage is crosscut by a second generation of dissolution-enhanced fractures filled by orange luminescent sparitic calcite (Fig. 4h). Non-planar anhedral dolomites are observed (Fig. 4g, h) and appear non-luminescent under CL (Fig. 4h).

In the Reculet Nord, the *Calcaires Récifaux* unit consists of a first reef sequence of about 10 m thickness, which is dolomitized throughout and characterized by an emersion surface at its top. This first sequence is followed by about 15 m of grainstone rich in gastropods, bivalves, and green algae on top of which a second reef sequence was deposited. The oolitic grainstone on top of the first reef sequence (Fig. 5a) is characterized by an important, partially replacive dolomitization affecting the interparticular space. These dolomite crystals are characterized by medium to coarse euhedral rhombs partly replacing the grains. Under CL (Fig. 5b), the dolomite displays a thick bright luminescent yellow to brown zoned core characterized by dissolution and followed by a bright luminescent red zoned core. Thick bladed isopachous cement rims are present around allochems (Fig. 5c) and a sparitic to micro-sparitic blocky calcite cement fills the interparticular space. Under cathodoluminescence, two stages of blocky calcite cementation can be distinguished: (1) a bright luminescent, orange zoned one and (2) a dull luminescent little to non-zoned one (Fig. 5d). Echinoderms fragments are surrounded by inclusion-rich, syntaxial overgrowth (Fig. 5e, f).

4.3 The Reef Complex units—*Calcaires de Landaize*

In all studied sections, this unit is characterized by limestone beds composed of a beige oncoid-rich grainstone with sparitic calcite cementation. The samples from Col de la Faucille, Valefin, and Roche Blanche sections share the same diagenetic features: (1) isopachous cement rims around allochems, syntaxial overgrowth around echinoderms fragments, and two successive stages of blocky

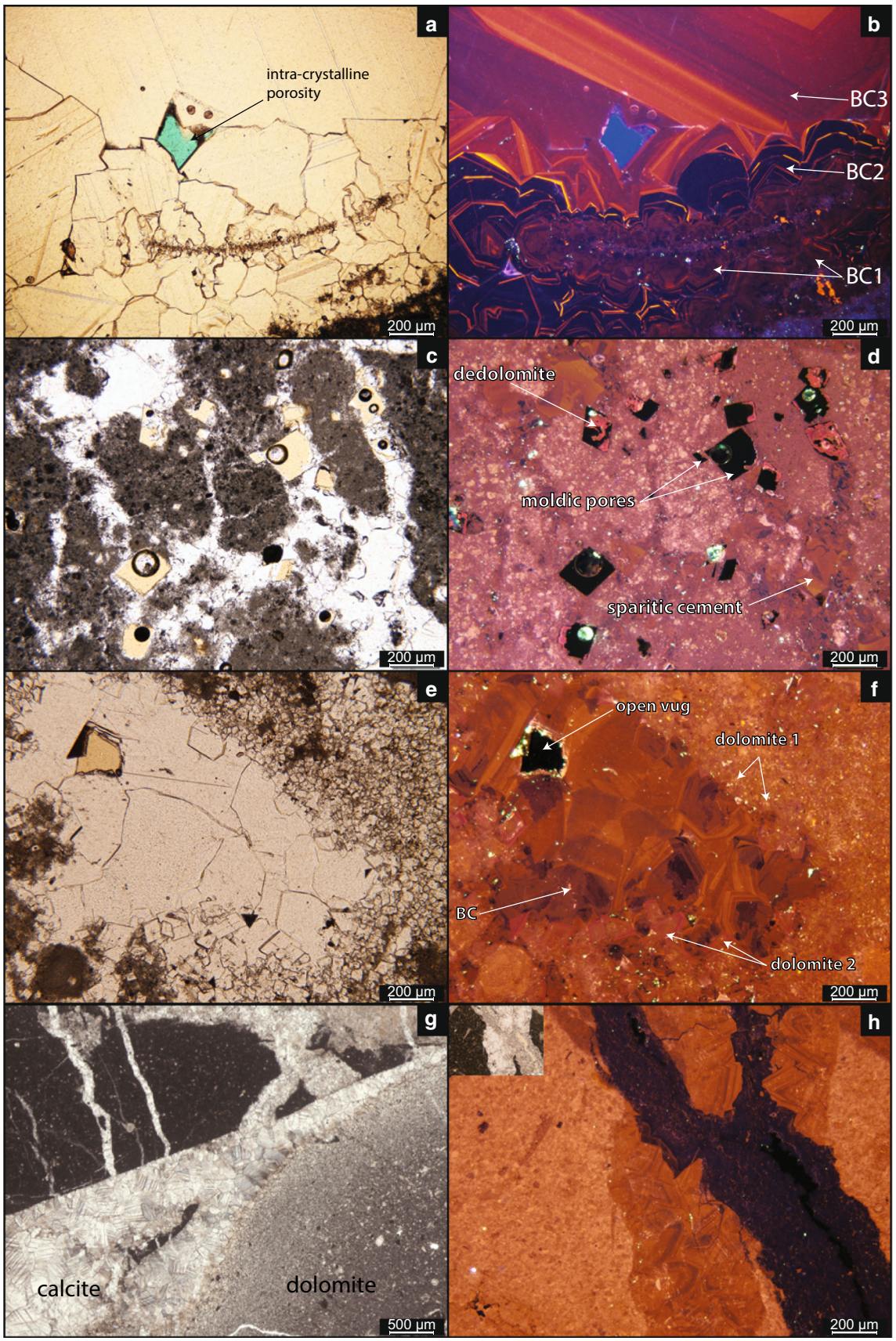
a
intra-crystalline
porosity
200 µm
b
BC3
BC2
BC1
200 µm
c
200 µm
d
dedolomite
moldic pores
sparitic cement
200 µm
e
200 µm
f
open vug
dolomite 1
BC
dolomite 2
200 µm
g
calcite
dolomite
500 µm
h
200 µm

◀**Fig. 4** Photomicrographs (optical microscope and cathodoluminescence) of the *Calcaires Récifaux* unit. **a**, **b** Multi-phased incomplete blocky calcite cementation leaving intra-crystalline porosity in the HU-2 well (sample YM49). **c**, **d** Dedolomitization as observed in the Prapont section (sample YM55). **e**, **f** Replacement planar dolomite overprinting pre-existing blocky calcite cementation in the Roche Blanche section (sample YM8). **g** Intensively fractured micritic limestone in the Champfromier section. The calcite filling the fracture exhibits thin twinning (sample YM14). **f** The same sample in natural light (top left) and under cathodoluminescence displaying a dissolution enhanced fracture filled by non-luminescent calcite

calcite cementation. No dolomite was observed in these sections. The Morillon section differs from the other sections in that isopachous cements are absent, grain interpenetration with pressure-dissolution sutures is common, and rhombohedral interparticular moldic pores are widespread (Fig. 5g, h).

Overall, the *Calcaires de Tabalcon* unit displays three dolomite phases. In the Etiollet section, most of the unit is firstly characterized by fine to medium replacive, euhedral dolomite followed by a fine to medium, euhedral to subhedral dolomite. In the Reculet Nord section, a third stage of medium to coarse, planar-euhedral, fabric-destructive dolomite is observed. Both the first and third stages display dedolomitization by calcitization. The *Calcaires Récifaux* unit is also affected by three distinct stages of dolomite. The two first phases are similar to those previously described in the Etiollet section. The third stage, present only in the grainstone facies in the Reculet Nord section is characterized by medium to coarse, euhedral dolomite partially replacing the margins of carbonate grains. Dedolomitization, either as calcitization or as dissolution of dolomite crystals, led to porogenesis in the *Calcaires Récifaux* unit. The *Calcaires de Landaize* unit is affected only by one stage of dolomitization in form of fine euhedral replacive dolomite associated to microstylolites located at the grain contact. Dedolomitized grains are common, resulting in rhomb-shaped moldic pores.

5 Paragenesis

5.1 Paragenesis of the *Calcaires de Tabalcon* unit

The paragenesis of this unit is the following (Fig. 6a): Micritization affecting skeletal fragments and particles as the earliest stage recorded. It is interpreted to occur mainly in shallow-marine environments and directly on, or just below, the seafloor (Bathurst 1966; Alexandersson 1972; Land and Moore 1980). Moldic porosity created by organic matter degradation and aragonite dissolution is filled by drusy calcite crystals. Syntaxial overgrowth, rarely observed, is limited to the bioclastic facies of the Salève site. The idiotopic texture of the dolomites with well-visible rhombs is indicative of dolomitization occurring during the "early" stages of diagenesis, at very shallow burial, with temperatures below 50 °C (Gregg and Sibley 1984). Overall, this replacement dolomite exhibits cloudy cores surrounded by limpid rims indicating that the cores developed from fluids evolving from a state of near saturation with low-Mg calcite in the early stages to a state of undersaturation (Nader et al. 2007; Sibley 1980; Warren 2000). This early dolomitization is followed by a first stage of blocky calcite cementation (BC1) which, under CL, displays zonation indicating chemical modifications of the parent fluids during crystallization (Meyers 1974; Machel 1985). A first stage of compaction affected this unit as evidenced by the compaction features affecting skeletal fragments (Fig. 3c), indicating that the moldic porosity was not entirely filled during compaction. Then the second stage of blocky calcite cementation (BC2) filled the remaining pore space when available. BC2 shows zonation under CL, which could indicate minor modification of the chemical composition of the fluid during precipitation or be the results of changing redox conditions. Therefore, the blocky calcite cementation took place in the open porosity during mesogenesis and burial. A stage of calcite-filled micro-fractures with bright yellow luminescence under CL affects all stages described so far. The sucrosic euhedral dolomite observed in the Reculet Nord represents an advanced stage of replacement which obliterated the original texture. Most of the dolomite is affected by calcitization associated with intercrystalline microvugs (Fig. 3d). This process could be driven by the migration of Ca-rich water through the unit, which led to a beginning of dedolomitization by partial dissolution and later infilling of created porosity by calcite cement in a two-step process (Ayora et al. 1998). A late stage of compaction associated with calcite-filled fractures crosscuts all previous stages (Fig. 6a).

5.2 Paragenesis of the Reef Complex units

The *Calcaires Récifaux* unit shares almost the same early diagenetic history with the *Calcaires de Tabalcon*, namely micritization, moldic dissolution, and syntaxial overgrowth (see paragenesis in Fig. 6b). The most important differences are the blocky calcite cementation and dolomitization. The *Calcaires Récifaux* in the HU2 core underwent an early stage of isopachous cementation followed by a first stage of dolomitization, three successive stages of blocky calcite cementation (see Fig. 4b), a second stage of dolomitization and dedolomitization. Dolomitization affected most of units, as observed both in outcrops

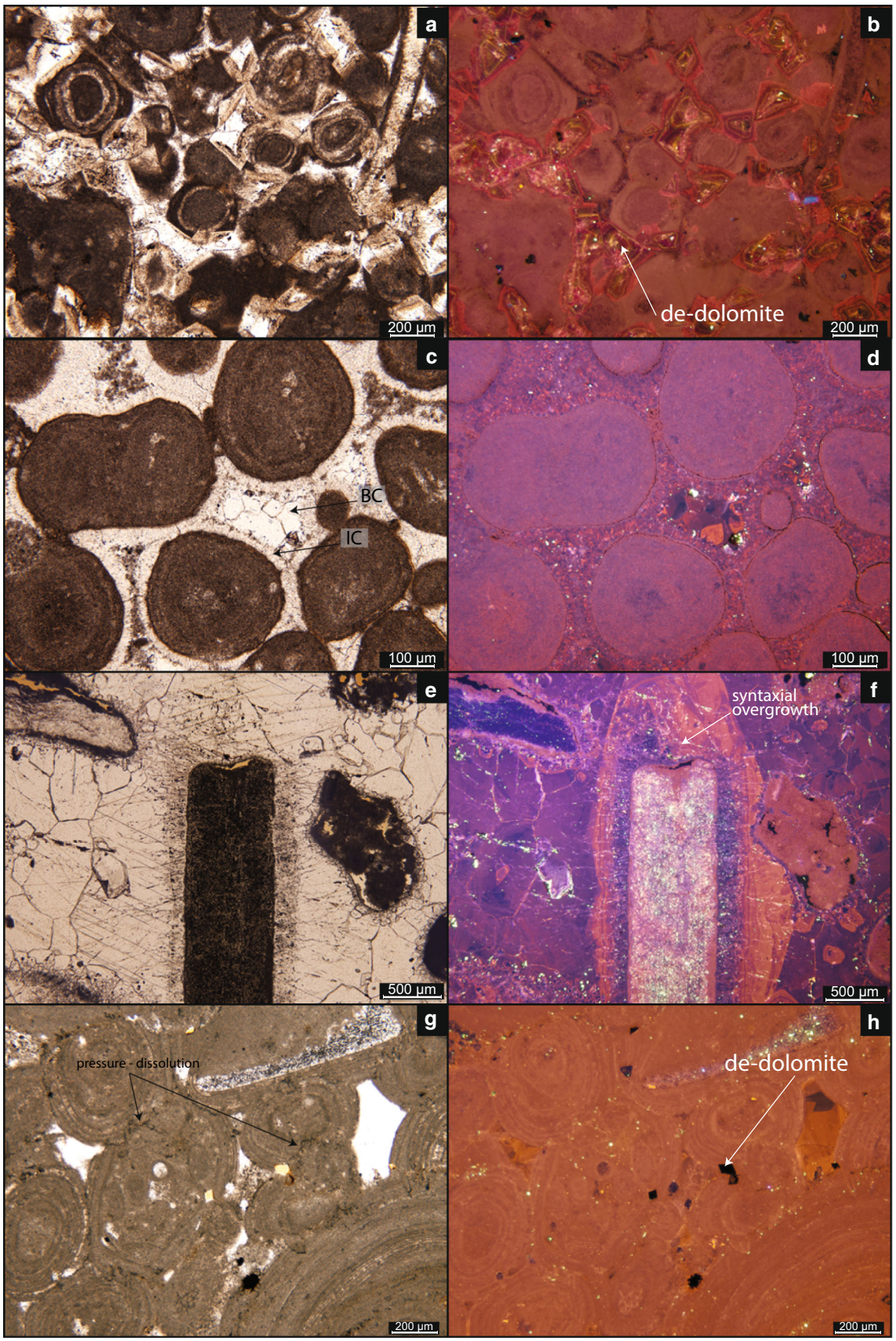
a
200 µm
b
de-dolomite
200 µm
c
BC
IC
100 µm
d
100 µm
e
500 µm
f
syntaxial overgrowth
500 µm
g
pressure - dissolution
200 µm
h
de-dolomite
200 µm

◀**Fig. 5** Photomicrographs (optical microscope and cathodoluminescence) of the *Calcaire Récifaux* and *Calcaires de Landaize* units. **a**, **b** Grainstone facies, as observed in the Reculet Nord section, showing replacement dolomite affected by calcitization with calcitized cores appearing orange and dolomite rims appearing red under CL (sample YM63). **c**, **d** grainstone facies in the Valefin section showing isopachous cement rim (IC) of allochems. The residual space is filled by blocky calcite (BC) cementation (sample YM2). **e**, **f** the same facies in the Roche Blanche section showing isopachous cementation and large syntaxial overgrowth around an echinoderm bioclast (sample YM6). **g**, **h** *Calcaires de Landaize* oolitic to oncoidic grainstone exhibiting important pressure-dissolution contact due to compaction. Under CL, the interparticular pore space is filled by blocky calcite cementation cross-cut by rhomboedral moldic pores due to dedolomitization (sample YM5)

(Reculet Nord, Prapont) and subsurface (as described in the non-cored interval in HU2). The occurrence of replacive planar euhedral dolomites with well visible rhombs, preferentially in the fore reef facies and more precisely replacing the micritic matrix, indicates that the dolomitization occurred during the "early" stages of diagenesis. All of the blocky cement stages show zonation indicative of important changes in the chemical composition of the parent fluid during precipitation. The mostly non-luminescent, strongly zoned second stage of blocky calcite cementation is interpreted as a result of meteoric diagenesis, involving water typically poor in Fe and Mn and continually fluctuating chemical conditions (Tucker and Wright 1990; Holail 1992). The latest stage of blocky calcite cementation (BC3) is incomplete and the initial porosity is preserved with intercrystalline macropores, lacking dissolution (Fig. 4b–e). In all other study sites, two stages of blocky calcite cements were identified, with a predominance of the second stage, BC2 (dull luminescent, brown to orange zonation under CL). This blocky calcite

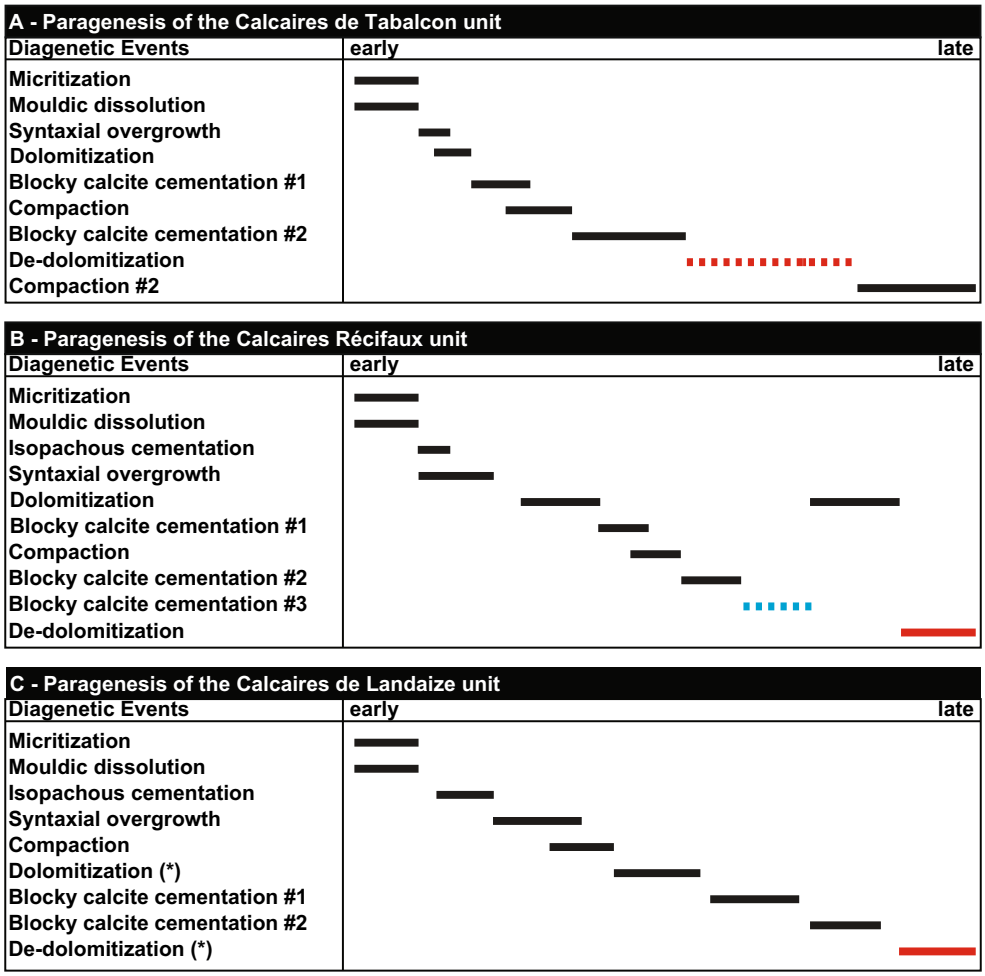

Fig. 6 Paragenesis of the *Calcaires de Tabalcon* unit (**a**), *Calcaires Récifaux* unit (**b**) and *Calcaires de Landaize* unit (**c**). Of the three units, the *Calcaires Récifaux* is the only one displaying a third stage of incomplete blocky calcite cementation. While all units were affected by dedolomitization, the degree of this process varies with only the *Calcaires Récifaux* and *Calcaires de Landaize* units exhibiting complete dedolomitization leading to the creation of secondary pore space. Asterisk indicate in the *Calcaires de Landaize* unit, dolomite and dedolomite occur only in the Morillon section

cementation most likely took place during mesogenesis under reducing conditions. This stage is followed by dedolomitization, almost similar to that previously described in the *Calcaires de Tabalcon* unit. Complete dedolomitization, enhanced by the important secondary, rhombohedral moldic porosity, is observed only in Prapont (Fig. 4c, d). Remnants of dolomite tend to be localized on the edge of the pores and exhibit large dissolution features. Dedolomitization may indicate the flow of Mg-depleted water leading to the dissolution of dolomite with minor or no precipitation of calcite (Ayora et al. 1998; Reinhold 1998; Kyser et al. 2002).

The paragenesis in Champfromier differs from that of other study sites. First, the depositional context in Champfromier is particular: the micritic limestone was deposited in a calm open marine environment probably due to a lower topography (Bernier 1984). Second, the limestone contains large, sparitic, calcite-filled fractures that are later affected by dolomitization. The presence of thin calcite twinning could indicate that the calcite infillings were affected by tectonic deformation, under a temperature below 140 °C (Burkhard 1993; Ferrill et al. 2004). Moreover, the fact that dolomitization is characterized by a non-planar anhedral texture indicates that the temperature during its precipitation was greater than 50 °C (Gregg and Sibley 1984; see discussion below). Therefore, it appears that the *Calcaires Récifaux* unit in Champfromier was affected by very late diagenesis through greater burial. Moreover, dissolution enhanced fractures, filled by non-luminescent blocky sparite, indicates very late meteoric dissolution/precipitation process after exhumation.

The paragenesis of the *Calcaires de Landaize* unit is comparable to that from the other studied sites (Fig. 6c). Early diagenesis is marked by micritization and isopachous cementation followed by moldic dissolution. The isopachous cementation forms a thick rim around allochems. This first stage of cementation occurred prior to or during early compaction as it can be observed trapped between particles or as rims around particles already in contact. Syntaxial overgrowth started at the same time because the isopachous cement precipitation around echinoderm fragments is not rimmed. Both the presence of isopachous cements and well developed syntaxial overgrowth most likely indicate a marine phreatic environment during the early stages of diagenesis (Land 1970; Longman 1980). The syntaxial overgrowth is followed immediately by the first stage of blocky calcite cementation (BC1) displaying a bright luminescence with orange zonation under CL and then a second stage (BC2). Only the Morillon section exhibits rhombohedral moldic porosity pointing to dedolomitization.

6 Discussion

6.1 Models of dolomitization

The processes and diagenetic environments involved in the precipitation of dolomite have been and are still debated due to the fact that dolomite is rarely observed in modern marine depositional environments, despite its abundance in ancient sedimentary rocks (Arvidson and Mackenzie 1999). The "dolomite problem" results from the poor understanding of the chemical and/or hydrological conditions of formation and the difficulty to propose a single genetic origin derived from petrographic and geochemical data (Machel 2004). The following discussion on dolomitization processes affecting the Upper Jurassic limestones of the Geneva Basin is based mostly on petrographic data taking into account the paragenetic interpretation of this study. The discussion on dolomitization models for the three types of dolomite described in this study is based on previous work and results from local and regional studies summarized in Tables 1, 2 and 3. The dolomitization occurring in the Champfromier section is clearly different from that observed in the other sites and will be discussed separately.

The first type of dolomite, exhibiting replacive euhedral rhombs mostly in a micritic matrix, fits well with a model of early reflux-type dolomitization (Adams and Rhodes 1960; Warren 2000; Machel 2004). The unimodal size distribution of the first dolomite indicates a single nucleation event while the idiotopic euhedral texture is indicative of a formation temperature below the critical roughening a temperature of 50 °C as defined by Gregg and Sibley (1984). The reflux-type model was proposed by Adams and Rhodes (1960) to explain extensive lagoonal and reefal dolomite in the Permian Basin of West Texas. In this model, the dolomitizing fluids are mesosaline brines with salinities controlled by surface evaporation in near-surface and shallow burial diagenetic settings. These brines originate from seawater evaporated beyond gypsum saturation in lagoonal and shallow-marine settings on a carbonate platform behind a reef acting as a barrier. The hypersaline brines, being denser than seawater, initiate downward fluid migration through the platform sediments, inducing dolomitization. This model is favored in the present case as the Kimmeridgian reef complex in the Geneva Basin developed in a marine, possibly protected, lagoonal zone (Meyer 2000). Moreover, the Prapont section includes, on top of the reef sequences, a succession of lagoonal and subtidal storm deposits, capped by supratidal mudflats and beach deposits (Fookes 1995). However two problems arise from this model in our study: (1) evidence for evaporite precipitation is lacking in the studied sections

Table 1 Examples of dolomitization reported throughout the Phanerozoic

References	Geological age	Locality	Formation	Type(s) and characteristics of dolomite(s)	Model(s)/Origin(s) of dolomitization
Iannace et al. (2014)	Early-Late Cretaceous	Southern Apennines, Italy	Mt. Faito and Mt. Chianello	1. Fine (~ 50 μm) 2. Fine to medium (~ 120 μm)—subhedral to euhedral—cloudy cores and clear rims	Few pulses of reflux of only slightly concentrated marine brines
Gomez-Rivas et al. (2014)	Early Cretaceous	Maestrat Basin, Spain	Benicassim	Fine to coarse—subhedral to anhedral—replacive fabric-retentive—cloudy	Hydrothermal dolomitization by thermal convection of concentrated seawater migrating per-ascencum from Permian–Triassic and/or Paleozoic basement, along major faults and permeable beds
Papaioanou and Carotsieris (1993)	Jurassic-Cretaceous	Central Peloponnesus, Greece	Tripoli unit	1. Unimodal—very fine to fine—euhedral 2. Polymodal—very-fine to fine—subhedral 3. Unimodal—medium—subhedral 4. Polymodal—medium to coarse—subhedral- void filling 5. Uni to polymodal—medium to coarse—euhedral 6. Polymodal—fine to medium—euhedral	1. Penecontemporaneous, supratidal replacive and/or direct precipitation 2. Mechanical introduction of dolomitic sediments 3. Replacement or neomorphism of type 1 dolomite during burial 4, 5, 6. Replacive dolomitization
Cervato (1990)	Jurassic-Cretaceous	Southern Alps, Italy	–	Fine grained to sucrosic with microamygdaloidal porosity	Hydrothermal dolomitization related to volcanic activity
Rustichelli et al. (2017)	Late Jurassic-Early Cretaceous	Gargano Promontory, S. Italy		Unimodal—medium to coarse—sub-euhedral and euhedral—limpid, cloudy, sometimes cloudy cores with limpid rims—fabric destructive	Fault-related dolomitization by modified seawater during shallow burial
Rameil (2008)	Late Jurassic-Early Cretaceous	NW Switzerland, France	Twannbach	1. Medium—euhedral to subhedral—cloudy cores and clear rims—replacive 2. Fine—euhedral—replacive 3. Fine to medium—subhedral	1. Reflux of dense hypersaline brines from evaporitic lagoons into the platform 2. Tidal/evaporitic pumping 3. Microbial mediation dolomitization of burrows 4. Dedolomitization during long-term emersion by meteoric waters
Reinhold (1998)	Late Jurassic	Swabian Alb, S. Germany	Lacunosmaergel Untere Felsenkalke Obere Felsenkalke	1. Fine to coarse—euhedral to anhedral—porphyrotopic—fabric selective to pervasive; idiotopic to xenotopic 2. Medium to very-coarse—subhedral to anhedral—pervasive; xenotopic 3. Medium to coarse—euhedral to anhedral—porphyrotopic to pervasive; idiotopic to xenotopic 4. Fine to coarse—euhedral to subhedral—void filling cement 5. Medium to coarse—anhedral—void filling, syntaxial cement 6. Fine to coarse—euhedral to anhedral—void filling cement	1. Early dolomitization during shallow burial by modified seawater 2. Two recrystallization phases of dolomite by: interaction with modified seawater or mixed meteoric/marine water during burial and then descending meteoric waters 3. Shallow burial dolomitization leading to dolomite and ferroan dolomite cements 4. Late shallow burial saddle dolomite cementation related to deep-burial hydrothermal fluids transported along reactivated fractures

Table 1 (continued)

References	Geological age	Locality	Formation	Type(s) and characteristics of dolomite(s)	Model(s)/Origin(s) of dolomitization
Baldermann et al. (2015)	Late Jurassic	N. German Basin, Germany	Langenberg section	1. Fine to medium—euhedral to subhedral 2. Fine to medium—euhedral to subhedral—hypidiotopic to idiotopic—fabric destructive—cloudy cores and clear rims 4. Coarse—euhedral—void filling cement—fabric retentive	Shallow seepage reflux and/or evaporitic tidal pumping at moderate temperatures (26 to 37 °C) by pristine marine to slightly evaporitic and reducing seawater derived interstitial solutions. Dolomitization was facilitated by bacterial sulfate reduction
Vincent (2001)	Late Jurassic	Paris Basin, France	Callovian-Oxfordian	Fine—idiotopic—cloudy cores	Associated to pressure/dissolution features Dewatering of Callovian-Oxfordian clays rich in Mg, Fe, and Mn

The selected cases, based on relevance for the present study, range from the Upper Jurassic to Upper Cretaceous, along with dolomite types reported, the model of dolomitization and the locality. Case studies contemporaneous, and/or close, to the sites studied in the present paper are highlighted in bold

and (2) the dolomitization is limited to decametric to metric thick beds instead of a massive body of dolomite. Rameil (2008) pointed out this issue in his study of Upper Jurassic and Lower Cretaceous limestones of north-west Switzerland, a few kilometers north-east of our study area. The lack of evaporite deposits could be explained by the fact that the dolomitizing fluids were mesosaline (below gypsum saturation) instead of hypersaline, as documented by Simms (1984), Kaufman (1994), and Machel (2004). Moreover, during periods of small and high-frequency sea-level changes, prograding platforms tends to develop into platform-top areas with large supratidal domains regularly inundated by storm surges (Montañez and Read 1992; Sun 1994; Rameil 2008; see also Gabellone and Whitaker 2016). In this case, mesosaline fluids could become the source of reflux-dolomitization, a scenario known as "brine reflux dolomitization" (Warren 2000) or "penesaline dolomitization" (Qing et al. 2001). The scenario proposed by Rameil (2008) is a two-step process. During high-sea level, hypersaline brines are limited to the tidal flat environment with recharges coming from storms and reflux limited to this zone. In the lagoon, while evaporation occurs, free water exchanges with seawater are possible as the platform rim is below sea level. Therefore, brines produced in the lagoon are stenonohaline to mesosaline only, without reflux in the intertidal domain. When the sea-level drops, the platform rim may be emerged, limiting the water exchange between the lagoon and open marine seawater. Evaporation in the lagoon will lead to the production of mesosaline to hypersaline fluids of higher density that will initiate a reflux-type dolomitization as they sink towards the platform rim. The hypothesis of Rameil (2008), based on the work of Mutti and Simo (1994) and Qing et al. (2001), proposes that pulses of dolomitizing fluids are responsible for the observed distribution of dolomite bodies. These pulses can be induced by repeated high-frequency sea-level falls where the next sea-level rise induces a latent reflux. This alternating reflux, dependent on the sea-level changes, would then result in repeated infiltration horizons creating repeated dolomitization in the peritidal limestone succession (Rameil 2008).

As pointed out by Fookes (1995) for the Prapont section, the lagoonal deposits were possibly affected by an increase in water salinity evidenced by a gradual decrease in abundance of green algae and foraminifera. This may have resulted in forming mesosaline fluids. In addition, high-frequency sea-level fluctuations were observed and described both in the Prapont (Fookes 1995) and Etiollet (Deville 1990) sections. The first type of dolomite exhibits replacive euhedral rhombs, mostly in a micritic matrix matching the criteria of matrix-selective dolomitization which is commonly the earliest stage of dolomitization (Machel 2004). While it is not clear if a critical roughening temperature exists for replacive dolomite (Braithwaite 1991; Machel 2004), Baldermann et al. (2015) reported a moderate temperature of about 26 °C for their first type of replacive dolomite in the Upper Jurassic limestone of the North German Basin. Therefore, data from the present study agree with the scenario of an early dolomitization in near-surface to shallow conditions, following a reflux-type model with mesosaline to hypersaline waters.

Table 2 Examples of dolomitization reported throughout the Phanerozoic

References	Geological age	Locality	Formation	Type(s) and characteristics of dolomite(s)	Model(s)/origin(s) of dolomitization
Moore et al. (1988)	Late Jurassic	NW Golf of Mexico	Smackover	1. Fine—pervasive—early 2. Coarse—replacive—cloudy cores and clear rims 3. Euhedral—pore filling	Evaporative reflux-meteoric water mixing model or recrystallization model by reflux in a meteoric water system. No unique conclusive scenario
Nader et al. (2007)	Late Jurassic	Central Lebanon	Bikfaya	1. Coarse (< 200 μm)- planar anhedral to subhedral 2. Very coarse (> 400 μm)—planar anhedral to euhedral—sometimes cloudy cores and clear rims 3. Coarse to very coarse (200 to 400 μm)—planar subhedral to euhedral 4. Fine to very coarse (50 to 600 μm)—planar subhedral to euhedral—cloudy cores and clear rims	1. Synsedimentary microbial dolomitization 2. Fault controlled hydrothermal dolomitization 3. Near surface mixing/meteoric dolomite dissolution 4. Deep burial dolomitization
Goldberg (1967)	Late Jurassic	Negeve, Southern Israel	HaMakhtesh HaQatan	Anhedral to hypidiotopic and idiotopic	Supratidal dolomitization, reflux of hypersaline water De-dolomitization related to subaerial exposure
Adabi (2009)	Late Jurassic	Kopet-Dagh Basin, N.E. Iran	Mozduran	1. Fine (∼ 40 μm)—subhedral 2. Medium (∼ 140 μm)—euhedral—replacive—cloudy core and clear rims 3. Medium (220 μm)—subhedral to anhedral—destructive 4. Coarse (∼ 500 μm)—anhedral 5. coarse—planar-C, often euhedral crystals—void filling cement	1. Replacement dolomite in supratidal to upper intertidal setting, near surface by seawater interactions 2. Shallow burial dolomite from dissolution of HMC 3. Shallow to intermediate burial 4. and 5. Deeper and maximum burial diagenesis
Wierzbicki et al. (2006)	Late Jurassic	Nova Scotia, Canada	Abenaki pf, Deep Panuke reservoir	Fine to medium—anhedral to subhedral—clear or cloudy cores and clear rims saddle—void-filling cement and replacive	Hydrothermal dolomitization during deep burial Hydrothermal dedolomitization
Barale et al. (2013)	Middle-Late Jurassic	Maritime Alps, Italy	Provençal and Subbriançonnais Units	1. Fine to medium—anhedral to subhedral—replacive 2. Coarse to very coarse—saddle—replacive—void filling cement	Several dolomitization pulses from hydrothermal fluids separated by hydrofractured processes
Bajestani et al. (2016)	Middle-Late Jurassic	Central Iran	Qal'eh Dokthar	1. Fine (30 μm)—subhedral—replacive 2. Medium (150 μm)—subhedral—cloudy cores 3. Medium (150 μm)—euhedral—cloudy cores and clear rims 4. Coarse (600 μm) subhedral—fabric destructive—cloudy cores and clear rims 5. Coarse (700 μm)—euhedral—fabric destructive 6. Coarse—void filling cement	1. Low temperature early dolomitization from seawater 2. and 3. Shallow burial dolomitization 4. and 5. Deep and maximal burial diagenesis, Mg source is diagenesis of clay and compaction of mudstone

Table 2 (continued)

References	Geological age	Locality	Formation	Type(s) and characteristics of dolomite(s)	Model(s)/origin(s) of dolomitization
Buchbinder et al. (1984)	Middle-Late Jurassic	Ashgod-Gan Yavne, Israel	Zohar and Shderot Formations	1. Large—anhedral—replacive 2. Fine to very coarse—euhedral to subhedral—replacive 3. Fine to medium—subhedral—replacive or cement	Dolomitization by a meteoric dominated fluid in a mixing zone or freshwater phreatic environment

The selected cases, based on relevance for the present study, range from the Middle to Upper Jurassic, along with dolomite types reported, the model of dolomitization and the locality

The second stage of dolomitization exhibits fine to medium, euhedral to subhedral dolomite rhombs. This second dolomite is thought to have originated from the same dolomitization event that led to the first stage of dolomitization but resulting in two dolomite populations (Machel 2004). This texture is characterized by two distinct types of dolomite with different sizes, shapes, pore types, and connectivity. The crystals of the smaller sized population has a cloudy core with or without clear rims. Domains with the larger sized dolomite exhibit higher intercrystalline porosity (Machel 2004). This is the case for the *Calcaires de Tabalcon* (Fig. 3e–f) and *Calcaires Récifaux* (Fig. 4e–f) units. Machel (2004) suggests two hypotheses for this texture, namely a single event of dolomitization or recrystallization of precursor dolomite. Textural differences in the host limestone or heterogeneous lithification prior to dolomitization can explain the difference in dolomite texture. The second hypothesis can be linked to near-surface or evaporitic dolomite originating from reflux-type dolomitization. Metastable protodolomite prone to recrystallization during burial results in some rock domains recrystallizing into a coarser texture. In our study, the recrystallization scenario is likely because the second dolomite is characterized by a coarser texture, crosscutting the first dolomite. However the timing of this second event is difficult to constrain. While Machel (2004) stated that recrystallization occurred during burial, no information is given on the depth of this burial. Given the petrographic data provided in the present study and in agreement with Reinhold (1998), the second generation of dolomite could originate from recrystallization in a shallow burial environment closely related to the first reflux-type dolomite.

The third stage of dolomitization was observed only in the Reculet Nord section. In the *Calcaires de Tabalcon* unit the sucrosic dolomite represents an advanced stage of replacement that obliterated the original fabric creating high intercrystalline porosity. The rhombs exhibit cloudy cores surrounded by rims. In the *Calcaires Récifaux* unit, the partially replacive, medium to coarse euhedral dolomite crosscuts pressure-dissolution features. These observations tend to give this third stage a more complex origin than the previous ones, likely due to burial dolomitization.

Several models exist for the generation and migration of dolomitizing fluid during burial. Heydari (1997) discriminated three categories or burial diagenesis realms in function of hydro-tectonic processes: passive margin, collision margin, and post-orogenetic. Machel (2004) proposes four different scenarios also based on the processes driving fluid flow: compaction, thermal convection, topography, and tectonically driven. For the present study, the data at hand can help to discard some of these scenarios for the Geneva Basin.

In the compaction (or passive margin) driven model, seawater or modified trapped seawater is buried with the sediment during burial and pumped due to compaction dewatering (Illing 1959; Jodry 1969). This process can produce only limited extent of dolomitization due to the limited amount of compaction water but is viable when the fluid is funneled towards small volumes of limestones. Choquette and Hiatt (2008) discussed the importance of shallow burial dolomite cement as a component of ancient sucrosic dolomite, describing this as "cements that were never deeply buried, are limpid, have planar faces (non-saddle forms), often distinct zonation in cathodoluminescence and form syntaxial overgrowth on crystals facing pores". The model proposed by Choquette and Hiatt (2008) is a four-step process common in lime mud (mudstone to wackestone textures), compatible with evaporitic dolomite. The first step represents the nucleus stage where dolomite crystals grow authigenically or are emplaced as detrital particles in the limestone, providing a very fine (1–10 μm) nucleus for the following step. During the second step, the cortex will grow around the nucleus, initiating the first stage of textural coarsening, replacing the initial limestone. This coarsening might lead to crystal interpenetration due to competition and/or compaction. Crystals may also appear cloudy due to residual inclusions. The third step starts after the depletion of sediment-sourced Mg and/or complete dissolution of remaining $CaCO_3$. In this step, limpid planar-euhedral cement precipitated by

Table 3 Examples of dolomitization reported throughout the Phanerozoic

Authors	Geological age	Locality	Formation	Type(s) and characteristics of dolomite(s)	Model(s)/origin(s) of dolomitization
Brigaud et al. (2009a)	Middle Jurassic	Paris Basin, France	Oolite miliaire inférieure, Calcaires à Polypiers	1. Medium—euhedral—cloudy cores and clear rims 2. Coarse—anhedral	1. Dewatering during compaction of clay-rich formations and expulsion of Mg2. Hydrothermal dolomitization by per-ascensum fluids from Triassic formations
Railsback and Hood (2001)	Early-Middle Jurassic	Atlas Mountains, Morocco	Ziz Valley	1. Clear or cloudy rhombs—void filling cement 2. Sub-euhedral to euhedral—cloudy cores—replacive—calcitized 3. Anhedral—clear cores replacive calcitized	Marine-meteoric mixing zone Influx of Mg-poor meteoric waters causing calcitization of dolomite
Qing et al. (2001)	Early Jurassic	Gibraltar	Gibraltar Limestone Formation	1. Fine ($\sim$ 50 μm)—subhedral to anhedral 2. Medium ($\sim$ 150 μm)—subhedral—cloudy cores and clear rims	Replacement dolomitization induced by penesaline seawater that refluxed during high- and low-frequency sea-level changes
Haas et al. (2014)	Late Triassic	Hungary	Transdanubian Range	1. Fine to medium—porphyrotopic—cloudy cores and clear rims 2. Fine—anhedral to subhedral—cloudy cores 3. Medium—euhedral to subhedral—cloudy cores and clear rims 4. Coarse—xenotopic—void filling	1. Synsedimentary microbial dolomitization 2. Early shallow burial dolomitization 3. Burial pervasive dolomitization 4. Saddle dolomite precipitation in fractures 5. dedolomitization after uplift and near-surface exposition
Beckert et al. (2015)	Early Permian	Central Oman	Saiq	1. Fine—subhedral 2. Fine to medium—subhedral—idiotopic to hypidiotopic—replacive 3. Medium to coarse—xenotopic—void filling	1. Seepage reflux of hypersaline fluids near surface to shallow burial dolomitization 2. Burial dolomitization with or without hydrothermal fluids 3. Dedolomitization by meteoric fluids
Gasparrini et al. (2006)	Late Carboniferous	Variscan Cantabrian, Spain	Bodon Unit	1. Medium—anhedral—replacive—fabric destructive 2. Coarse—xenotopic—void filling	Burial, convective flow dolomitization by hydrothermal and hypersaline brines, possibly marine-derived
Gawthorpe (1987)	Early Carboniferous	Bowland Basin, N. England	Pendleside Limestone	1. Medium—anhedral to subhedral—cloudy cores and clear rims—replacive 2. Medium to coarse—subhedral, euhedral to anhedral—idiotopic to xenotopic—replacive 3. Fine—anhedral to subhedral—replacive—pore filling 4. Medium to coarse—subhedral to euhedral—cloudy cores and clear rims 5. Coarse—anhedral—replacive 6. Coarse—anhedral hypidiotopic to xenotopic—replacive and pore filling	Fault-related fracturing dolomitization from fluids saturated in Fe and Mg as a results of clay minerals transformations together with maturation of organic matter

Table 3 (continued)

Authors	Geological age	Locality	Formation	Type(s) and characteristics of dolomite(s)	Model(s)/origin(s) of dolomitization
Guo et al. (2016)	Early Ordovician–Late Cambrian	Tarim Basin, China	Lower Qiulit, Penglaiba, Yingshan	1. Fine—anhedral to subhedral 2. Fine to medium—euhedral to subhedral—cloudy cores and clear rim 3. Fine to coarse—anhedral—poikilotopic—fabric destructive—cloudy with rare clear rims 4. Fine to medium—euhedral to subhedral—cloudy core and clear rim 5. Coarse—xenotopic	1. Penecontemporaneous to near-surface dolomitization at low temperatures mediated by microbes, precipitated from slightly modified brines 2. Shallow burial dolomitization by seawater in association with burial dissolution 3. Recrystallization or neomorphism upon previous dolomite 4. and 5. Hydrothermal dolomitization from per-ascencum migrating fluids along fracture/fault conduits

The selected cases, based on relevance for the present study, range from the Lower Ordovician to Middle Jurassic, along with dolomite types reported, the model of dolomitization and the locality. We refer to appendix 1 of Choquette and Hiatt (2008) for an extended database

overgrowing over the cortex formed in step two. The initial fabric is completely obliterated, leaving important intercrystalline water-filled pore while the rigid framework formed by the dolomite cement tends to slow compaction. The last step consists of further overgrowth of dolomite cement filling the available pore space, leading to coarsening of the initial dolomite texture as long as pore space is available. The third stage of dolomitization seems to follow to a certain extent this scenario as the *Calcaires de Tabalcon* unit still displays important intercrystalline porosity, meaning that step three was the last step occurring. Following this reasoning, the third stage in the *Calcaires Récifaux* unit could also originate from shallow burial dolomitization without complete obliteration of the original fabric. This is supported by the fact that dolomite crystals crosscut the interpenetration and resulting microstylolitization of grains. These pressure-solution features are known to occur very early during burial at depth ranging from 60 to 90 m (Schlanger 1963; Dunnington 1967). Moreover, several studies assumed that cement dolomitization occurred in a relatively closed system with a local source of Mg-rich fluids (Murray 1960; Weyl 1960; Warren 2000). This scenario agrees with that of Choquette and Hiatt (2008), as these processes "may go to completion after relatively early, shallow burial (tens to hundreds of meters burial depths), at relatively low diagenetic temperatures". The thermal convection models are driven by spatial variations in temperature, due to elevated heat flux in the vicinity of igneous intrusions, lateral contrast between warm platforms waters and cold ocean waters, or lithology-controlled variations in thermal conductivity. This elevated heat flux will results in modification of the pore-water density (Kohout et al. 1977; Wilson et al. 1990). Two types of convection may form: open convection when the carbonate platform is open so seawater recharge laterally and discharge at the top; close convection if the temperature gradient is high enough with regards to the permeability of the limestone and in the absence of interbedded aquitards. While this model could be considered, there is no evidence that the requirement for an open or closed convection was met in the Kimmeridgian platform. Moreover, Machel (2004) reported that thermal convection can be "overpowered" by the presence of a reflux flow due to evaporitic waters, based on numerical modeling (Jones et al. 2002, 2003, 2004).

The tectonic or collision margin model (Oliver 1986; Heydari 1997; Warren 2000; Machel 2004) requires hot (100 °C to above 250 °C), metamorphic or hypersaline and highly pressured fluids, driven towards the basin margin and vertically through faults and fractures. Such hot fluid are responsible for non-planar and saddle dolomite precipitation. The dolomitization in the Champfromier section is the only one that contrasts the most with that observed in other sections studied. In this section, dolomitization seems to be associated with faults and fracturing. In addition the thin calcite twining is indicative of the calcite infillings affected by tectonic deformation (see above). The fact that dolomitization is characterized by a non-planar texture indicates that the temperature during its precipitation was greater than 50 °C (Gregg and Sibley 1984). Moreover, Radke and Mathis (1980) and Gregg (1983) postulated formation temperatures greater than 60 °C, which is in line with fluid inclusion data on saddle dolomites from the Upper Jurassic at the Franconian Alb, southeast Germany, which document precipitation temperatures between 60 and 90 °C (Liedmann and Koch 1990; Liedmann 1992). All of these observations support the assumption of deeper burial, where dolomitization would be the results of tectonic or hydrothermal driven fluids. The important overprint of tectonics in this section makes the paragenesis

reconstruction more difficult to assess. Until further work is done on this section, no predominant scenario for dolomitization can be unequivocally privileged.

In the topography or post-orogenetic model (Tóth 1988; Garven 1995; Heydari 1997; Warren 2000; Machel 2004), dolomitization is considered as the result of an important amount of meteoric water migrating in uplifted sedimentary basins through recharge zones. During migration, the meteoric fluid will dissolve Mg-rich material prior to reaching the limestone where dolomitization will occur. The topography model does not appear to be common and only few examples were reported from the Cambrian carbonates in Missouri (Gregg 1985), the Cambrian-Ordovician carbonates in southern Canadian Rocky Mountains (Yao and Demicco 1995), and more recently from the Upper Cretaceous carbonates in the Dead Sea Transform, central Negev desert (Matthews et al. 2006). The active tectonics responsible for thrusting and folding of the Jura took place recently, in a time period ranging from the Miocene to the Pliocene (Laubscher 1986, 1992; Maurer et al. 1997; Sommaruga 1997; Burkhard and Sommaruga 1998; Mosar 1999; Becker 2000) while the Jura and Salève Mountains exhumation could have started as early as the Eocene (Schroeder 1958). A dolomitization following this scenario would occur later than the one resulting from compaction as discussed previously. Therefore, this model is not considered to explain neither early nor burial dolomitization observed in the present study. However, this process might have induced further dolomitization of buried rocks in the basin after exhumation. This issue is discussed further in Sect. 6.3.

6.2 Comparison with existing models

The bibliography on dolomitization is extensive, with various models available since the very first description of dolomite (de Dolomieu 1791). The objective of this section is not to review all previous studies. We selectively summarize some examples of dolomitization in limestones from the Lower Ordovician to the Upper Cretaceous, mostly in the Tethys realm (Tables 1, 2). Examples are presented along with a summary of the different stages of dolomitization, the respective pathways and scenarios invoked. Below, we focus on case studies from the Upper Jurassic and/or from areas close to the Geneva Basin. Reinhold (1998) published a thorough study dealing with the dolomitization of the Kimmeridgian formations in the Swabian platform (South Germany). The stratigraphic levels are equivalent to the Lower and Upper Kimmeridgian deposits in the Geneva Basin. Reinhold (1998) described six types of diagenetic dolomites. The first dolomite type displays rhombs that are fine to coarse, idiotopic euhedral to xenotopic anhedral, porphyrotopic, and fabric selective to pervasive. He interpreted this first stage as the result of an early dolomitization during shallow burial induced by modified seawater. The next two stages are quite similar and exhibit medium to (very) coarse rhombs that can be euhederal, subhedral to anhedral, and pervasive. This second and third stages are linked to two recrystallization phases of dolomite by an interaction with modified seawater or mixed meteoric/marine water during burial followed by downward migration of meteoric waters. The fourth and fifth stages are dolomite cements characterized by a first fine to coarse, euhedral to subhedral void filling cement directly followed by medium to coarse anhedral void filling syntaxial dolomite. These stages were interpreted as being the result of shallow burial dolomitization. The last stage is represented by fine to coarse, euhedral to anhedral void filling cements in the form of saddle dolomite being the results of late shallow burial related to deep-burial hydrothermal fluids transported along reactivated fractures. While Reinhold (1998) does not consider a reflux-type model, the timing of dolomitization is similar to that of the present study, with a first early stage followed by shallow burial dolomitization. The fourth and fifth stages exhibit the same characteristics as those of this study's third stage in the form of a void filling and syntaxial dolomitization that could be the result of a scenario similar to that described in Choquette and Hiatt (2008). Moreover, the last stage of deep-burial dolomitization could be similar to that described in the Champfromier section with dolomitization associated with fluid circulation along fractures. Rameil (2008) studied the Upper Jurassic–Lower Cretaceous Twannbach formation in northwest Switzerland, a few kilometers to 50 km away from sites presented in the present study, and reported three diagenetic dolomites. The first stage displays medium euhedral to subhedral replacive rhombs exhibiting cloudy cores and clear rims. The second stage is characterized by a fine euhedral replacive dolomite. The third is composed of fine to medium subhedral rhombs observed only in burrows. The processes linked to the generation of the first two generations of our study are similar to those of Rameil (2008). The third stage of dolomitization is interpreted as microbial mediation where burrowing organisms induces biochemical modifications by concentrating organic matter that in turn will serve as a substrate for bacterial colonization. Under reducing conditions, sulphate-reducing bacteria would consume SO_4^{2-}, which acts as an inhibitor to dolomite precipitation as it may bind with Mg^{2+} resulting in lower Mg/Ca ratio. In such a context, dolomitization by microbial mediation can occur. Furthermore, Rameil (2008) reported two types of dedolomite which he interpreted as the result of long-term emersion and interaction with meteoric waters. This dedolomitization scenario is similar to that recorded and presented in

this study. Baldermann et al. (2015) focused on dolomitization of the Upper Jurassic Langenberg section in the North German Basin (Germany). The authors distinguished three stages of dolomitization: a first stages represented by fine to medium, euhedral to subhedral, dolomite; a second, displaying fine to medium, euhedral to subhedral, hypidiotopic to idiotopic fabric destructive dolomite exhibiting cloudy cores and clear rims; and a third stage exhibiting coarse euhedral void filling cements which are fabric retentive. Baldermann et al. (2015) interpreted these dolomitization events as the results of shallow seepage reflux and/or evaporitic tidal pumping at moderate temperatures (26° to 37 °C) by pristine marine to slightly evaporitic and reducing seawater derived from interstitial solutions. As for the Swabian platform (Reinhold 1998), dolomitization is thought to have been facilitated by bacterial sulfate reduction. In addition, the last stage of dolomitization is affected by dedolomitization. Data and interpretations of Baldermann et al. (2015) are very similar to those presented in this study, indicating that the processes leading to dolomitization and dedolomitization of the Upper Jurassic in the Geneva Basin and in the North German Basin might be related. The dolomitization processes reported in Reinhold (1998), Rameil (2008), and Baldermann et al. (2015) are very similar to those described in this paper. Textural characteristics of the different stages of dolomite in all studies described above are analogs to those recorded in the Upper Jurassic limestones in the Geneva Basin. Specifically the second stage of fabric destructive dolomite in the North German Basin (Baldermann et al. 2015) which is almost identical to the sucrosic dolomite reported in the third stage of our study. Therefore, a reflux-type model of dolomitization followed by syntaxial overgrowth during shallow burial, as suggested for the Geneva Basin, appears to apply to most cases reported so far for the Upper Jurassic from northern Switzerland up to the North German Basin (Table 1). Dolomitization is scarce in basins close to the Geneva Basin. In their study of the Upper and Middle Jurassic limestones in the Paris Basin, Vincent (2001) and Brigaud et al. (2009b) reported dolomite associated with stylolites and fractures. Both studies proposed that dolomitization was either the consequence of dewatering during compaction of clay-rich formation, providing Mg-rich fluids (most probably from the Callovian-Oxfordian clays) and/or a result upward migrating hydrothermal fluids from Triassic. Such a scenario is also reported from Middle Jurassic to Lower Cretaceous limestones in Italy where most of the dolomitization is thought to be associated to hydrothermal fluids and fault-related processes (Cervato 1990; Barale et al. 2013; Rustichelli et al. 2017). Other examples of such models of dolomitization were reported from Spain, from the Upper Carboniferous limestones of the Bodon unit (Variscan Cantabrian) (Gasparrini et al. 2006) and the Lower Cretaceous limestones of the Benicassim formation (Masetrat Basin) (Gomez-Rivas et al. 2014). Iannace et al. (2014) showed that the Lower–Upper Cretaceous limestones in the South Apennines of Italy (Mt. Faito and Mt. Chianello sections) were affected by two stages of dolomitization. These stages resulted from several pulses of "slightly" concentrated marine brines, similar to the scenarios of Rameil (2008). Farther from the Geneva Basin, a significant number of studies dealing with dolomitization in limestones with stages, textures, and characteristics comparable to those described in the present work were conducted. Some of these are discussed below. Readers can refer to Tables 1, 2 and 3 for references and detailed characteristics of dolomitization and their associated models in the Upper Jurassic and other time intervals.

Other studies in the Upper Jurassic exhibit data and interpretations fairly similar to those of this study. Goldberg (1967) showed that the Upper Jurassic limestones in the Negev of Southern Israel were affected by supratidal dolomitization due to a reflux of hypersaline water. This dolomite is then affected by a stage of dedolomitization probably related to subaerial exposure. In the North-West Golf of Mexico, Moore et al. (1988) showed that the Upper Jurassic limestones are affected by three stages of dolomitization (early pervasive then coarse replacive and pore filling dolomites) which are the results of an evaporative reflux-water scenario. In North East Iran, the Upper Jurassic limestones display five stages of dolomitization (coarsening from 40 to 500 μm) that are the result of a supratidal to upper intertidal seawater dolomitization followed by shallow burial dolomitization (Adabi 2009). Similar examples were reported from other time intervals, e.g., in the Lower Permian limestones of Central Oman where Beckert et al. (2015) described three stages of dolomitization resulting from seepage reflux of hypersaline fluids and shallow burial dolomitization. These dolomites were also affected by dedolomitization, probably due to meteoric fluids.

6.3 Implications for future subsurface prospection and exploitation

Assessing the potential of carbonate reservoirs is not easy because of their inherent heterogeneities. Limestones of the Geneva Basin are no exception as the diagenetic history proved to be complex with processes partly overriding precedent diagenetic phases. Nevertheless, the studied units revealed promising reservoir qualities, especially in the sucrosic dolomite where porosity values can range from 10 to 15% and permeability can reach 35 mD (Moscariello 2016; Rusillon et al. 2016). Dolomitization has an important impact on reservoir properties as it is often associated

with increase in porosity and permeability, especially in sucrosic dolomites (e.g., Schmoker et al. 1985; Warren 2000; Wang et al. 2015; Giorgioni et al. 2016). In such sucrosic facies, the high intercrystalline porosity can form a highly connected porous network ensuring good fluid flow, storage and drainage properties. However, over-dolomitization in shallow burial settings, as discussed in Choquette and Hiatt (2008), can lead to an important decrease in porosity and, thus, possibly contribute to reducing reservoir properties. In the same way, dedolomitization can produce important amount of secondary porosity, also having important impacts on reservoir properties. Therefore the estimation of the volume of dolomitized limestone in the subsurface is very important in the actual plan to produce geothermal energy in the Geneva Basin. For such an estimate, it is necessary to constrain the volume of dolomitizing fluid migrating through the basin and quantify the extent of dedolomitization.

The scarcity of subsurface data is a major pitfall to estimate the volume of dolomitizing fluids in the basin. In the Humilly-2 (Hu-2) well, no cores or cuttings of dolomitized limestone are available, therefore only the non-published final drilling report can provide some insights. According to the report, the Upper Jurassic limestone exhibits two dolomitized intervals: one from 1181 to 1271 m (TVD) displaying a "beige limestone locally dolomitized with layers of darkened sucrosic dolomite" and one from 949 to 1009 m (TVD) displaying a "beige, fine to coarse limestone with presence of coarse, gray, compact dolomitic limestone". Therefore we can roughly estimate that about 150 m of limestones are affected by dolomitization in Hu-2. The hônex-1 well (Th-1) is located 17.5 km east of Hu-2. Only two cores were recovered, one in the Lower Cretaceous and one in the Tidalites de Vouglans unit (Fig. 1). Here also, the non-published final drilling report is the only source of information. In this well, the final drilling report mentioned that the reef complex is about 216.6 m thick but dolomite was only observed at the base of the *Calcaires de Tabalcon* unit (2038 m depth). However, fractures are abundant and calcite filled according to the report. The unit underlying the *Calcaires de Tabalcon* seems to have fractures filled by dolomitic cements. The absence of dolomitization in the Th-1 well is rather interesting and unexpected. Indeed it is not unusual to find replacive texture present in a single formation and locally even in a single outcrop or thin section (Warren 2000). Without available cores or cuttings it is difficult to provide further discussion about the absence of dolomite in this well.

While the present study proposed that the dolomitization was an early process, a scenario of late dolomitization that may have affected the subsurface of the Geneva Basin cannot be excluded. First of all, the Jura Mountains are subject to active tectonics since the Miocene. Therefore, some questions arise: could topographic driven dolomitization affect the subsurface? Most of the dolomite is affected by calcitization which can be driven by meteoric fluid migrating through the limestone during telogenesis after exhumation (Ayora et al. 1998; Kyser et al. 2002). This could lead to Mg-enriched fluids possibly migrating toward the basin. As the Upper Jurassic is currently acting as an aquifer in the subsurface, such fluids could act as recharge water and possibly induce further dolomitization. Moreover, the Molasse Basin was affected by a decollement horizon in the thick Triassic evaporites (Philippe 1994). Compactional fluids originating from tectonic squeezing, as expected in a tectonic-driven scenario, are a viable alternative. The same applies for Mg-rich fluids originating from dewatering of clay-rich layers during compaction (Vincent 2001; Vincent et al. 2007; Brigaud et al. 2009a, b). Moreover, the northern part of the Geneva Basin is affected by four major wrench faults representing potential high-intensity fracture zones with associated enhanced permeability conditions (Clerc et al. 2015). In this context, hydrothermal driven fluids migrating upward could also be considered, which would fit the occurrence of dolomitic cements filling fractures in the Th-1 well.

Although some conclusions can be made from the present study, some issues remain open, particularly regarding diagenetic processes in the basin center. To better understand and constrain the volume and extension of the dolomitization, additional cores need to be acquired. Furthermore, the acquisition of geochemical data on the dedolomitization by sampling the remaining dedolomite will provide fundamental data to constrain and evaluate the type and timing of fluids that led to the calicization of the dolomitic Upper Jurassic limestones.

7 Conclusion

The Upper Jurassic carbonate rocks form a complex carbonate reservoir strongly affected by dolomitization and dedolomitization. This study provides a relative chronology of diagenetic stages for the different units present in the Kimmeridgian of the Geneva Basin. Based on the petrographic data acquired from sub-surface cores and outcrops, the following conclusions can be made:

1. Most of the initial porosity in the different units studied was filled by blocky calcite cement. This cementation occurred during early burial diagenesis. Most of units exhibit a two-stage blocky calcite cementation and only the top of the *Calcaires Récifaux* evidences a third incomplete stage of blocky calcite

cementation with preservation of intracrystalline macroporosity.

2. Dolomitization occurred during early diagenesis and overprinted all precedent stages. The most affected units are the *Calcaires de Tabalcon* and the *Calcaires Récifaux*. To some extent, the *Calcaires de Landaize* unit is affected but only in the Morillon section. In most cases, dolomite has a planar, non-mimicking replacive texture.
3. Petrographic data was used to assess the dolomitization scenarios. The first stages of dolomitization are interpreted to be induced by a reflux-type model involving mesosaline to hypersaline fluid originating from evaporitic conditions in a lagoonal environment. High-frequency sea-level fluctuations acted as a mechanism for pulse migration of the brines through the limestone resulting in partial dolomitization. The second stage of dolomitization is thought to result from recrystallization during shallow burial. The third stage of replacive, fabric-destructive dolomite is explained by shallow burial dolomitization generating syntaxial overgrowth dolomite over pre-existing nuclei. This process is responsible for the highly porous sucrosic dolomite occurring in the Reculet section.
4. Dedolomitization is identified at different order of magnitude by either: (1) almost complete dissolution leading to the creation of secondary pore space or (2) two-step calcitization driven by the infiltration of Ca-rich water leading to dissolution, formation of micro-vugs, and secondary precipitation of calcite.
5. The creation of secondary pore space could provide good connectivity between the intraparticular or matrix related microporous network and the interparticular moldic macroporous network. This enhanced connectivity could therefore provide good reservoir properties suitable for geothermal energy exploitation.

As for most studies, carbonate heterogeneity remains to be a major issue when assessing the exploitation potential. Understanding the paragenesis affecting such reservoirs is an important step towards the better exploitation of resources currently available. This study provides further insights on a possible reflux driven dolomitization occurring in shallow carbonate platforms.

Acknowledgements This work was funded by the SIG (Services Industriels de Genève) as a part of the GEothermy 2020 project. We would like to thank Carsten Reinhold (Rhein Petroleum, Germany) and Anneleen Foubert (Fribourg, Switzerland) for their constructive suggestions. We thank François Gischig, Nino Isabella Valenzi and Agathe Martignier from the Department of Earth Sciences, University of Geneva, Switzerland, for their help with thin sections manufacturing, thin section staining, and S.E.M. imaging, respectively. We thank Patrick Marques (Total) and Damien DoCouto (University of Geneva) for organizing the Humilly-2 core display at the Total core library (Boussens, France). Jérôme Chablais (HydroGeo, Geneva) and Nicolas Clerc (GESDEC, Geneva) were helpful in the field.

References

Adabi, M. H. (2009). Multistage dolomitization of upper Jurassic Mozduran Formation, Kopet-Dagh Basin, N.E. Iran. *Carbonates and Evaporites, 24*(1), 16–32. https://doi.org/10.1007/BF03228054.

Adams, J. E., & Rhodes, M. L. (1960). Dolomitization by seepage refluxion. *AAPG Bulletin, 44*(12), 1912–1920.

Alexandersson, T. (1972). Micritization of carbonate particles: Processes of precipitation and dissolution in modern shallow-marine sediments. *Universitet Uppsala, Geologiska Institut Bulletin, 7*(3), 201–236.

André, F. (1962). Etude paléontologique de la formation récifale de Plagne (Ain). Ph.D. dissertation, Université Pierre et Marie Curie, Paris 6, France.

Arvidson, R. S., & Mackenzie, F. T. (1999). The dolomite problem; control of precipitation kinetics by temperature and saturation state. *American Journal of Science, 299*(4), 257–288.

Ayora, C., Taberner, C., Saaltink, M. W., & Carrera, J. (1998). The genesis of dedolomites: a discussion based on reactive transport modeling. *Journal of Hydrology, 209*(1–4), 346–365.

Bajestani, M. S., Mahboubi, A., Al-Aasm, I., Moussavi-Harami, R., & Nadjafi, M. (2016). Multistage dolomitization in the Qal'eh Dokhtar Formation (Middle-Upper Jurassic), Central Iran: petrographic and geochemical evidence: Dolomitization in the Qal'eh Dokhtar Fm. *Geological Journal, 53,* 22–44. https://doi.org/10.1002/gj.2876.

Baldermann, A., Deditius, A. P., Dietzel, M., Fichtner, V., Fischer, C., Hippler, D., et al. (2015). The role of bacterial sulfate reduction during dolomite precipitation: Implications from Upper Jurassic platform carbonates. *Chemical Geology, 412,* 1–14.

Barale, L., Bertok, C., d'Atri, A., Domini, G., Martire, L., & Piana, F. (2013). Hydrothermal dolomitization of the carbonate Jurassic succession in the Provençal and Subbriançonnais Domains (Maritime Alps, North-Western Italy). *Comptes Rendus Geoscience, 345*(1), 47–53. https://doi.org/10.1016/j.crte.2012.10.015.

Bathurst, R. G. C. (1966). Boring algae, micrite envelopes and lithification of molluscan biosparites. *Geological Journal, 5*(1), 15–32.

Becker, A. (2000). The Jura Mountains—an active foreland fold-and-thrust belt? *Tectonophysics, 321*(4), 381–406.

Beckert, J., Vandeginste, V., & John, C. M. (2015). Exploring the geological features and processes that control the shape and internal fabrics of late diagenetic dolomite bodies (Lower Khuff equivalent–Central Oman Mountains). *Marine and Petroleum Geology, 68,* 325–340.

Bernier, P. (1984). Les formations carbonatées du Kimméridgien et du Portlandien dans le Jura méridional: stratigraphie, micropaléontologie, sédimentologie. Ph.D. dissertation, Université de Lyon, Laboratoire de Géologie, Lyon, France.

Bernier, P., & Enay, R. (1972). Figures d'émersion temporaire et indices de sédimentation à très faible profondeur dans le Portlandien et le Kimméridgien supérieur (Calcaires en plaquettes) du Grand-Colombier-de-Culoz (Ain, France). *Bulletin de la Société Géologique de France, 7*(1–5), 281–292.

Braithwaite, C. J. R. (1991). Dolomites, a review of origins, geometry and textures. *Earth and Environmental Science Transactions of The Royal Society of Edinburgh, 82*(2), 99–112.

Brigaud, B., Durlet, C., Deconinck, J.-F., Vincent, B., Pucéat, E., Thierry, J., et al. (2009a). Facies and climate/environmental

changes recorded on a carbonate ramp: A sedimentological and geochemical approach on Middle Jurassic carbonates (Paris Basin, France). *Sedimentary Geology, 222*(3–4), 181–206.

Brigaud, B., Durlet, C., Deconinck, J.-F., Vincent, B., Thierry, J., & Trouiller, A. (2009b). The origin and timing of multiphase cementation in carbonates: Impact of regional scale geodynamic events on the Middle Jurassic Limestones diagenesis (Paris Basin, France). *Sedimentary Geology, 222*(3), 161–180. https://doi.org/10.1016/j.sedgeo.2009.09.002.

Burkhard, M. (1993). Calcite twins, their geometry, appearance and significance as stress-strain markers and indicators of tectonic regime: A review. *Journal of Structural Geology, 15*(3–5), 351–368.

Burkhard, M., & Sommaruga, A. (1998). Evolution of the western Swiss Molasse basin: Structural relations with the Alps and the Jura belt. *Geological Society, London, Special Publications, 134*(1), 279–298.

Carozzi, A. V. (1950). "Graded bedding" et rythmes de sédimentation dans le Séquanien supérieur du Grand-Salève (Haute-Savoie). *Archives des Sciences Genève, 3,* 439–442.

Carozzi, A. V. (1954). Le Jurassique supérieur récifal du Grand-Salève, essai de comparaison avec les récifs coralliens actuels. *Eclogae Geologicae Helvetiae, 47,* 373–446.

Carozzi, A. V. (1955). Sédimentation récifale rythmique dans le Jurassique supérieur du Grand-Salève (Haute-Savoie, France). *Geologische Rundschau, 43*(2), 433–446.

Cervato, C. (1990). Hydrothermal dolomitization of Jurassic-Cretaceous limestones in the southern Alps (Italy): Relation to tectonics and volcanism. *Geology, 18*(5), 458–461. https://doi.org/10.1130/0091-7613(1990)018<0458:HDOJCL>2.3.CO;2.

Charollais, J., Davaud, E., & Jamet, M. (1996). Evolution du bord oriental de la plate-forme jurassienne entre le Jurassique supérieur et l'Oligocène: modèle basé sur trois forages pétroliers (Haute-Savoie). *Géologie de la France, 1,* 25–42.

Charollais, J.-J., Weidmann, M., Berger, J.-P., Engesser, B., Hotellier, J.-F., Gorin, G. E., et al. (2007). La Molasse du bassin franco-genevois et son substratum. *Archives des Sciences Genève, 60,* 59–174.

Charollais, J., Wernli, R., Mastrangelo, B., Metzger, J., Busnardo, R., Clavel, B., et al. (2013). Présentation d'une nouvelle carte géologique du Vuache et du Mont de Musieges (Haute-Savoie, France). Stratigraphie et tectonique. *Archives des Sciences Genève, 66,* 1–64.

Choquette, P. W., & Hiatt, E. E. (2008). Shallow-burial dolomite cement: a major component of many ancient sucrosic dolomites. *Sedimentology, 55*(2), 423–460.

Clerc, N., Rusillon, E., Moscariello, A., Renard, P., Paolacci, S., & Meyer, M. (2015). Detailed structural and reservoir rock typing characterisation of the Greater Geneva Basin, Switzerland, for geothermal resource assessment. In *World geothermal congress, Melbourne, Australia, 19–25 April*.

Davis, J. M., Roy, N. D., Mozley, P. S., & Hall, J. S. (2006). The effect of carbonate cementation on permeability heterogeneity in fluvial aquifers: An outcrop analog study. *Sedimentary Geology, 184*(3), 267–280. https://doi.org/10.1016/j.sedgeo.2005.11.005.

de Dolomieu, D. (1791). Sur un genre de pierres calcaires très peu effervescentes avec les acides et phosphorescentes par la collision. *Journal de Physique, 39,* 3–10.

Debelmas, J., & Michel, R. (1961). Silicifications par altération climatique dans les séries alpines. *Travaux du Laboratoire de Géologie de la Faculté des Sciences de Grenoble, 37,* 7–14.

Deville, Q. (1988). Analyse sédimentologique et séquentielle des terrains les plus anciens du Salève: les traces d'un récif à la base (?) du Kimméridgien. *Archives des sciences Genève, 40,* 65–84.

Deville, Q. (1990). Chronostratigraphie et lithostratigraphie synthétique du Jurassique supérieur et du Crétacé inférieur de la partie méridionale du Grand Saleve (Haute-Savoie, France). *Archives des Sciences Genève, 43,* 215–235.

Dickson, J. A. D. (1966). Carbonate identification and genesis as revealed by staining. *Journal of Sedimentary Research, 36*(2), 491–505.

Disler, C. (1914). Stratigraphie und Tektonik des Rotliegenden und der Trias beiderseits des Rheins zwinschen Rheinfelden und Augst, Ph.D. dissertation, Universität Basel, Basel, Switzerland.

Dou, Q., Sun, Y., & Sullivan, C. (2011). Rock-physics-based carbonate pore type characterization and reservoir permeability heterogeneity evaluation, Upper San Andres reservoir, Permian Basin, west Texas. *Journal of Applied Geophysics, 74*(1), 8–18. https://doi.org/10.1016/j.jappgeo.2011.02.010.

Dunnington, H. V. (1967). Aspects of diagenesis and shape change in stylolitic limestone reservoirs (pp. 339–352). In: *7th World petroleum congress, Mexico City, Mexico, 2–9 April*.

Ehrenberg, S. N., & Nadeau, P. H. (2005). Sandstone vs. carbonate petroleum reservoirs: A global perspective on porosity-depth and porosity-permeability relationships. *AAPG bulletin, 89*(4), 435–445.

Enay, R. (1965). Les formations coralliennes de Saint-Germain-de-Joux (Ain). *Bulletin de la Société géologique de France, 7*(1), 23–31.

Enay, R. (1969). Le prétendu" Argovien" d'Entremont (Haute-Savoie). Découverte de la zone à Platynota (Kimméridgien inférieur) au Vuache (Jura méridional). *Société de Physique et d'Histoire Naturelle de Genève, 4*(1), 68–76.

Favre, J. A., Risler, E., & Lossier, L. (1880). Description géologique du canton de Genève. A. Cherbuliez.

Ferrill, D. A., Morris, A. P., Evans, M. A., Burkhard, M., Groshong, R. H., & Onasch, C. M. (2004). Calcite twin morphology: A low-temperature deformation geothermometer. *Journal of Structural Geology, 26*(8), 1521–1529. https://doi.org/10.1016/j.jsg.2003.11.028.

Fondeur, C., Gottis, M., Rouire, J., & Vatan, A. (1954). Quelques aspects de la dolomitisation au Jurassique en France. *XIXème Congrès de Géologie International, Alger, 15,* 471–491.

Fookes, E. (1995). Development and eustatic control of an Upper Jurassic reef complex (Saint Germain-de-Joux, Eastern France). *Facies, 33*(1), 129.

Gabellone, T., & Whitaker, F. (2016). Secular variations in seawater chemistry controlling dolomitization in shallow reflux systems: Insights from reactive transport modelling. *Sedimentology, 63*(5), 1233–1259. https://doi.org/10.1111/sed.12259.

Garven, G. (1995). Continental-scale groundwater flow and geologic processes. *Annual Review of Earth and Planetary Sciences, 23*(1), 89–117. https://doi.org/10.1146/annurev.ea.23.050195.000513.

Gasparrini, M., Bechstädt, T., & Boni, M. (2006). Massive hydrothermal dolomites in the southwestern Cantabrian Zone (Spain) and their relation to the Late Variscan evolution. *Marine and Petroleum Geology, 23*(5), 543–568. https://doi.org/10.1016/j.marpetgeo.2006.05.003.

Gawthorpe, Robert L. (1987). Burial dolomitization and porosity development in a mixed carbonate-clastic sequence: An example from the Bowland Basin, northern England. *Sedimentology, 34*(4), 533–558. https://doi.org/10.1111/j.1365-3091.1987.tb00785.x.

Giorgioni, M., Iannace, A., D'Amore, M., Dati, F., Galluccio, L., Guerriero, V., et al. (2016). Impact of early dolomitization on multi-scale petrophysical heterogeneities and fracture intensity of low-porosity platform carbonates (Albian-Cenomanian, southern Apennines, Italy). *Marine and Petroleum Geology, 73,* 462–478.

Goldberg, M. (1967). Supratidal dolomitization and dedolomitization in Jurassic rocks of Hamakhtesh Haqatan, Israel. *Journal of Sedimentary Research, 37*(3), 760–773.

Gomez-Rivas, E., Corbella, M., Martín-Martín, J. D., Stafford, S. L., Teixell, A., Bons, P. D., et al. (2014). Reactivity of dolomitizing fluids and Mg source evaluation of fault-controlled dolomitization at the Benicàssim outcrop analogue (Maestrat basin, E Spain). *Marine and Petroleum Geology, 55,* 26–42. https://doi.org/10.1016/j.marpetgeo.2013.12.015.

Gregg, J. M. (1983). On the formation and occurrence of saddle dolomite—discussion. *Journal of Sedimentary Research, 53*(3), 1025–1026.

Gregg, J. M. (1985). Regional epigenetic dolomitization in the Bonneterre Dolomite (Cambrian), southeastern Missouri. *Geology, 13*(7), 503–506. https://doi.org/10.1130/0091-7613(1985)13<503:REDITB>2.0.CO;2.

Gregg, J. M., & Sibley, D. F. (1984). Epigenetic dolomitization and the origin of xenotopic dolomite texture. *Journal of Sedimentary Research, 54*(3), 908–931.

Guo, C., Chen, D., Qing, H., Dong, S., Li, G., Wang, D., et al. (2016). Multiple dolomitization and later hydrothermal alteration on the Upper Cambrian–Lower Ordovician carbonates in the northern Tarim Basin, China. *Marine and Petroleum Geology, 72,* 295–316. https://doi.org/10.1016/j.marpetgeo.2016.01.023.

Gygi, R. A. (2013). Integrated Stratigraphy of the Oxfordian and Kimmeridgian (Late Jurassic) in northern Switzerland and adjacent southern Germany. *Memoir of the Swiss Academy of Science, 104,* 150.

Haas, J., Budai, T., Győri, O., & Kele, S. (2014). Multiphase partial and selective dolomitization of Carnian reef limestone (Transdanubian Range, Hungary). *Sedimentology, 61*(3), 836–859.

Heim, A. (1922). Le sondage pour la recherche du pétrole à Challex (Ain). *Eclogae Geologicae Helvetiae, 17*(1), 115–123.

Heydari, E. (1997). Hydrotectonic models of burial diagenesis in platform carbonates based on formation water geochemistry in North American sedimentary basins. In I. P. Montanez, J. M. Gregg, & K. L. Shelton (Eds.), *Basin-wide diagenetic patterns: Integrated petrologic, geochemical, and hydrologic considerations*, *SEPM Special publication. 57*, 53–79. https://doi.org/10.2110/pec.97.57.0053.

Holail, H. (1992). Coordinated petrography-isotopic-chemical investigation of meteoric calcite cement (Jurassic-Pleistocene). *Egypt. Carbonates and Evaporites, 7*(1), 48–55. https://doi.org/10.1007/BF03175392.

Iannace, A., Frijia, G., Galluccio, L., & Parente, M. (2014). Facies and early dolomitization in Upper Albian shallow-water carbonates of the southern Apennines (Italy): Paleotectonic and paleoclimatic implications. *Facies, 60*(1), 169–194. https://doi.org/10.1007/s10347-013-0362-4.

Illing, L. V. (1959). Deposition and Diagenesis of some upper palaeozoic carbonate sediments in Western Canada. In *5th World petroleum congress, New York, USA, 30 May*.

Jodry, R. L. (1969). Growth and dolomitization of Silurian reefs, St. Clair County, Michigan. *AAPG Bulletin, 53*(4), 957–981.

Jones, G. D., Smart, P. L., Whitaker, F. F., Rostron, B. J., & Machel, H. G. (2003). Numerical modeling of reflux dolomitization in the Grosmont platform complex (Upper Devonian), Western Canada sedimentary basin. *AAPG Bulletin, 87*(8), 1273–1298.

Jones, G. D., Whitaker, F. F., Smart, P. L., & Sanford, W. E. (2002). Fate of reflux brines in carbonate platforms. *Geology, 30*(4), 371–374. https://doi.org/10.1130/0091-7613(2002)030<0371:FORBIC>2.0.CO;2.

Jones, G. D., Whitaker, F. F., Smart, P. L., & Sanford, W. E. (2004). Numerical analysis of seawater circulation in carbonate platforms: II. The dynamic interaction between geothermal and brine reflux circulation. *American Journal of Science, 304*(3), 250–284. https://doi.org/10.2475/ajs.304.3.250.

Joukowsky, E., & Favre, J. (1913). Monographie géologique et paléontologique du Salève (Haute Savoie). *Mémoire de la Société de Physique et d'Histoire Naturelle de Genève, 37,* 295–523.

Kaufman, J. (1994). Numerical models of fluid flow in carbonate platforms: Implications for dolomitization. *Journal of Sedimentary Research, 64*(1), 128–139.

Kohout, F. A., Henry, H. R., & Banks, J. E. (1977). Hydrogeology related to geothermal conditions of the Floridan Plateau. *Florida Bureau of Geology Special Publication, 21,* 1–34.

Kyser, T. K., James, N. P., & Bone, Y. (2002). Shallow burial dolomitization and dedolomitization of cenozoic cool-water limestones, Southern Australia: Geochemistry and origin. *Journal of Sedimentary Research, 72*(1), 146–157. https://doi.org/10.1306/060801720146.

Land, L. S. (1970). Phreatic versus vadose meteoric diagenesis of limestones: evidence from a fossil water table. *Sedimentology, 14*(3–4), 175–185. https://doi.org/10.1111/j.1365-3091.1970.tb00191.x.

Land, L. S., & Moore, C. H. (1980). Lithification, micritization and syndepositional diagenesis of biolithites on the Jamaican island slope. *Journal of Sedimentary Research, 50*(2), 357–369.

Laubscher, H. P. (1986). The eastern Jura: Relations between thin-skinned and basement tectonics, local and regional. *Geologische Rundschau, 75*(3), 535–553. https://doi.org/10.1007/BF01820630.

Laubscher, H. P. (1992). Jura kinematics and the Molasse Bassin. *Eclogae Geologicae Helvetiae, 85*(3), 653–675.

Liedmann, W. (1992). Diagnetische Entwicklung süddeutscher Malmkarbonate: unter Berücksichtigung lumineszenzpetrographischer, fluid inclusion und geochemischer Untersuchungsmethoden; Tabellen. Ph.D. dissertation, Universität Heidelberg, Heidelberg, Germany, 307p.

Liedmann, W., & Koch, R. (1990). Diagenesis and fluid inclusions of Upper Jurassic sponge-algal reefs in SW Germany. *Facies, 23*(1), 241. https://doi.org/10.1007/BF02536715.

Longman, M. W. (1980). Carbonate diagenetic textures from nearsurface diagenetic environments. *AAPG Bulletin, 64*(4), 461–487.

Machel, H.-G. (1985). Cathodoluminescence in calcite and dolomite and its chemical interpretation. *Geoscience Canada, 12*(4), 139–147.

Machel, H.-G. (1987). Saddle dolomite as a by-product of chemical compaction and thermochemical sulfate reduction. *Geology, 15*(10), 936–940. https://doi.org/10.1130/0091-7613(1987)15<936:SDAABO>2.0.CO;2.

Machel, H. G. (2004). Concepts and models of dolomitization: A critical reappraisal. *Geological Society, London, Special Publications, 235*(1), 7–63.

Matthews, A., Erel, Y., Listovsky, N., Grosz, S., Ayalon, A., Avni, Y., et al. (2006). Topographic- and density-driven fluids as sources of iron mineralization and dolomitization adjacent to the Dead Sea Transform. *Geochimica et Cosmochimica Acta, 70*(18, Supplement), A400. https://doi.org/10.1016/j.gca.2006.06.807.

Maurer, H. R., Burkhard, M., Deichmann, N., & Green, A. G. (1997). Active tectonism in the central Alps: contrasting stress regimes north and south of the Rhone Valley. *Terra Nova, 9*(2), 91–94. https://doi.org/10.1111/j.1365-3121.1997.tb00010.x.

Meyer, M. (2000). Le Complexe récifal Kimméridgien—Tithonien du Jura méridional interne (France), évolution multifactorielle, stratigraphique et tectonique. *Terre et Environment, 24,* 1–179.

Meyers, W. J. (1974). Carbonate cement stratigraphy of the Lake Valley Formation (Mississippian) Sacramento Mountains, New Mexico. *Journal of Sedimentary Petrology, 44*(3), 837–861.

Montañez, I. P., & Read, J. F. (1992). Eustatic control on early dolomitization of cyclic peritidal carbonates: Evidence from the Early Ordovician Upper Knox Group, Appalachians. *GSA*

Bulletin, 104(7), 872–886. https://doi.org/10.1130/0016-7606(1992)104<0872:ECOEDO>2.3.CO;2.

Moore, C. H., Chowdhury, A., & Chan, L. (1988). Upper Jurassic Smackover platform dolomitization northwestern Gulf of Mexico: A tale of two waters. *Sedimentology and Geochemistry of Dolostones, 43,* 753–778.

Mosar, J. (1999). Present-day and future tectonic underplating in the western Swiss Alps: Reconciliation of basement/wrench-faulting and décollement folding of the Jura and Molasse basin in the Alpine foreland. *Earth and Planetary Science Letters, 173*(3), 143–155. https://doi.org/10.1016/S0012-821X(99)00238-1.

Moscariello, A. (2016). Geothermal exploration in SW Switzerland. In *European Geothermal Congress, Strasbourg, France, 19–24 April*.

Mouchet, P. O. J. (1998). Stratigraphy and mineralostratigraphy of the Kimmeridgian in the central Jura mountains of Switzerland and eastern France. *Eclogae Geologicae Helvetiae, 91*(1), 53–68.

Mountjoy, E. W., & Marquez, X. M. (1997). Predicting reservoir properties in dolomites: Upper Devonian Leduc buildups, deep Alberta basin. *AAPG Memoir, 69,* 267–306.

Murray, R. C. (1960). Origin of porosity in carbonate rocks. *Journal of Sedimentary Research, 30*(1), 59–84.

Mutti, M., & Simo, J. A. (1994). Distribution, petrography and geochemistry of early dolomite in cyclic shelf facies, Yates Formation (Guadalupian), Capitan Reef Complex, USA. *Dolomites A Volume in Honour of Dolomieu International Association of Sedimentologists Special Publications, 21,* 91–107. https://doi.org/10.1002/9781444304077.ch7.

Nader, F. H., Swennen, R., Ellam, R. M., & Immenhauser, A. (2007). Field geometry, petrography and geochemistry of a dolomitization front (Late Jurassic, central Lebanon). *Sedimentology, 54*(5), 1093–1120.

Oliver, J. (1986). Fluids expelled tectonically from orogenic belts: Their role in hydrocarbon migration and other geologic phenomena. *Geology, 14*(2), 99–102. https://doi.org/10.1130/0091-7613(1986)14<99:FETFOB>2.0.CO;2.

Papaioanou, F. P., & Carotsieris, Z. (1993). Dolomitization patterns in Jurassic-Cretaceous dissolution-collapse breccias of Mainalon Mountain (Tripolis Unit, Central Peloponnesus-Greece). *Carbonates and Evaporites, 8*(1), 9–22. https://doi.org/10.1007/BF03175159.

Pelletier, M. (1953). Observations stratigraphiques sur les formations coralligènes du Bugey (Ain). *Comptes Rendus de l'Académie des Sciences, 237*(23), 1540–1542.

Philippe, Y. (1994). Transfer zone in the Southern Jura thrust belt (Eastern France): Geometry, development, and comparison with analogue modeling experiments. In A. Mascle (Ed.), *Hydrocarbon and petroleum geology of France* (pp. 327–346). Berlin: Springer. https://doi.org/10.1007/978-3-642-78849-9_23.

Qing, H., Bosence, D. W., & Rose, E. P. (2001). Dolomitization by penesaline sea water in Early Jurassic peritidal platform carbonates, Gibraltar, western Mediterranean. *Sedimentology, 48*(1), 153–163.

Radke, B. M., & Mathis, R. L. (1980). On the occurrence and formation of saddle dolomite. *Journal of Sedimentary Petrology, 50,* 1149–1168.

Railsback, L. B., & Hood, E. C. (2001). A survey of multi-stage diagenesis and dolomitization of Jurassic limestones along a regional shelf-to-basin transect in the Ziz Valley, Central High Atlas Mountains, Morocco. *Sedimentary Geology, 139*(3), 285–317. https://doi.org/10.1016/S0037-0738(00)00164-0.

Rameil, N. (2008). Early diagenetic dolomitization and dedolomitization of Late Jurassic and earliest Cretaceous platform carbonates: a case study from the Jura Mountains (NW Switzerland, E France). *Sedimentary Geology, 212*(1–4), 70–85.

Reinhold, C. (1998). Multiple episodes of dolomitization and dolomite recrystallization during shallow burial in Upper Jurassic shelf carbonates: eastern Swabian Alb, southern Germany. *Sedimentary Geology, 121*(1–2), 71–95.

Rong, H., Jiao, Y., Wu, L., Gu, Y., Zhang, L., Li, R., et al. (2012). Effects of diagenesis on the acoustic velocity of the Triassic oolitic shoals in the Yudongzi outcrop of Erlangmiao area, Northwest Sichuan Basin. *Journal of Earth Science, 23*(4), 542–558. https://doi.org/10.1007/s12583-012-0274-1.

Rusillon, E., Clerc, N., Brentini, M., & Moscariello, A. (2016). Rock typing, structural characterization and stratigraphy harmonization in support of geothermal exploration in the Greater Geneva Basin (Switzerland) (pp. 19–24). In *European geothermal congress, Strasbourg, France, 19–24 April*.

Rustichelli, A., Iannace, A., Tondi, E., Di Celma, C., Cilona, A., Giorgioni, M., et al. (2017). Fault-controlled dolomite bodies as palaeotectonic indicators and geofluid reservoirs: New insights from Gargano Promontory outcrops. *Sedimentology, 64*(7), 1871–1900. https://doi.org/10.1111/sed.12378.

Schlanger, S. O. (1963). Subsurface geology of Eniwetok atoll. *Geological Survery professional paper, 260*(BB), 991–1066.

Schmoker, J. W., Krystinik, K. B., & Halley, R. B. (1985). Selected characteristics of limestone and dolomite reservoirs in the United States. *AAPG Bulletin, 69*(5), 733–741.

Schroeder, J.-W. (1958). Géologie du pays de Genève. *Le Globe. Revue genevoise de géographie, 97,* 49–87.

Sibley, D. F. (1980). Climatic control of dolomitization, Seroe Domi Formation (Pliocene), Bonaire, N. A. *Special Publication of SEPM, 28,* 247–258.

Simms, M. (1984). Dolomitization by groundwater-flow system in carbonate platforms. *Gulf Coast Association of Geological Societies Transactions, 34,* 411–420.

Sommaruga, A. (1997). Geology of the central Jura and the Molasse Basin: New insight into an evaporite-based foreland fold and thrust belt. *Mémoire de la Société Neuchâteloise des Sciences Naturelles, 12,* 176. **(isbn: 2-88347-001-4)**.

Strasser A. (1994). Milankovitch cyclicity and high-resolution sequence stratigraphy in lagoonal–peritidal carbonates (Upper Tithonian–Lower Berriasian, French Jura Mountains). In *Orbital Forcing and Cyclic Sequences P.L. de Boer, D.G. Smith. Special Publication International Association of Sedimentologists* (pp. 285–301).

Strasser, A., Pittet, B., & Hug, W. (2015). Palaeogeography of a shallow carbonate platform: The case of the Middle to Late Oxfordian in the Swiss Jura Mountains. *Journal of Palaeogeography, 4*(3), 251–268. https://doi.org/10.1016/j.jop.2015.08.005.

Sun, S. Q. (1994). A reappraisal of dolomite abundance and occurrence in the Phanerozoic. *Journal of Sedimentary Research, 64*(2a), 396–404.

Tóth, J. (1988). Ground water and hydrocarbon migration. *Hydrogeology The Geological Society of North America, Boulder Colorado, O*(2), 251–268.

Tucker, M. E., & Wright, V. P. (1990). *Carbonate Sedimentology* (p. 482). Oxford: Blackwell.

Vincent, B. (2001). Sédimentologie et géochimie de la diagenèse des carbonates: application au Malm de la Bordure Est du Bassin de Paris. Ph.D. dissertation, Université de Bourgogne, Dijon, France.

Vincent, B., Emmanuel, L., Houel, P., & Loreau, J.-P. (2007). Geodynamic control on carbonate diagenesis: Petrographic and isotopic investigation of the Upper Jurassic formations of the Paris Basin (France). *Sedimentary Geology, 197*(3), 267–289. https://doi.org/10.1016/j.sedgeo.2006.10.008.

Walls, R. A., & Burrowes, G. (1985). The Role of cementation in the diagenetic history of Devonian reefs. *Western Canada. Special Publications of SEPM, 36,* 185–220.

Wang, G., Li, P., Hao, F., Zou, H., & Yu, X. (2015). Dolomitization process and its implications for porosity development in dolostones: A case study from the Lower Triassic Feixianguan Formation, Jiannan area, Eastern Sichuan Basin, China. *Journal of Petroleum Science and Engineering, 131,* 184–199. https://doi.org/10.1016/j.petrol.2015.04.011.

Warren, J. (2000). Dolomite: occurrence, evolution and economically important associations. *Earth-Science Reviews, 52*(1–3), 1–81.

Westphal, H., Eberli, G. P., Smith, L. B., Grammer, G. M., & Kislak, J. (2004). Reservoir characterization of the Mississippian Madison Formation, Wind River basin, Wyoming. *AAPG Bulletin, 88*(4), 405–432. https://doi.org/10.1306/12020301029.

Weyl, P. K. (1960). Porosity through dolomitization: conservation-of-mass requirements. *Journal of Sedimentary Petrology, 30*(1), 85–90.

Wierzbicki, R., Dravis, J. J., Al-Aasm, I., & Harland, N. (2006). Burial dolomitization and dissolution of Upper Jurassic Abenaki platform carbonates, Deep Panuke reservoir, Nova Scotia. *Canada. AAPG Bulletin, 90*(11), 1843–1861. https://doi.org/10.1306/03200605074.

Wilson, M. E. J., & Evans, M. J. (2002). Sedimentology and diagenesis of Tertiary carbonates on the Mangkalihat Peninsula, Borneo: Implications for subsurface reservoir quality. *Marine and Petroleum Geology, 19*(7), 873–900. https://doi.org/10.1016/S0264-8172(02)00085-5.

Wilson, E. N., Hardie, L. A., & Phillips, O. M. (1990). Dolomitization front geometry, fluid flow patterns, and the origin of massive dolomite: The Triassic Latemar buildup, northern Italy. *American Journal of Science, 290*(7), 741–796.

Yao, Q., & Demicco, R. V. (1995). Paleoflow patterns of dolomitizing fluids and paleohydrogeology of the southern Canadian Rocky Mountains: Evidence from dolomite geometry and numerical modeling. *Geology, 23*(9), 791–794. https://doi.org/10.1130/0091-7613(1995)023<0791:PPODFA>2.3.CO;2.